Building and Environment 222 (2022) 109393

Contents lists available at ScienceDirect

Building and Environment

journal homepage: www.elsevier.com/locate/buildenv

Moisture-resilient performance of concrete basement walls – Numerical simulations of the effect of outward drying

Silje Kathrin Asphaug [a,*], Erlend Andenæs [a], Stig Geving [b], Berit Time [b], Tore Kvande [a]

[a] Norwegian University of Science and Technology (NTNU), Department of Civil and Environmental Engineering, NO-7491, Trondheim, Norway
[b] SINTEF Community, Department of Architecture, Materials and Structures, NO-7465, Trondheim, Norway

ARTICLE INFO

Keywords:
Hygrothermal simulation
Outward drying
Concrete
Vapour-permeable thermal insulation
Dimpled membrane
Liquid transfer coefficient
Air flow

ABSTRACT

The moisture safety designs of basements used for habitation have become a topic of concern. Basements are prone to high moisture strain and have a limited outward drying ability compared with above-grade structures. The risk of interior moisture-related damage can be reduced if the basement walls are allowed to dry outward below grade. The use of vapour-permeable thermal insulation and the effect of air gaps behind dimpled membranes on the outward drying of concrete basement walls were investigated in this study. One- and two-dimensional hygrothermal simulations were conducted using WUFI®Pro and COMSOL Multiphysics®. First, the outward drying of concrete wall segments, previously investigated in a laboratory experiment, was simulated. Two EPS types and two dimpled membrane positions were compared, with an emphasis on the airflow through the air gap behind the membrane. Second, the long-term moisture performance of concrete basement walls was simulated. It was observed that when the dimpled membrane was placed between the concrete and exterior EPS, the bottom of the concrete segments dried faster than the top. When the dimpled membrane was placed on the exterior side, the concrete dried more uniformly along the height. Thus, the results indicated that the latter ensured outward drying of the concrete basement walls. However, the overall effect on the interior RH depended on the characteristics of concrete and the amount of interior and exterior insulation. Optimum drying was achieved when the thickness of interior insulation was reduced. The variability of the concrete properties used in basement walls requires further investigation.

1. Introduction

1.1. Habitable basements

In many Nordic countries, basements cover a significant share of the building volume. Traditionally, basements have been used for food storage; however, owing to population growth, rising house prices, and housing shortages, basements are often fitted out to a high standard and used as a living space. In sloped terrains, semi-basements (also referred to as daylight basements, English basements, or walk-out basements) are commonly used for habitation. Bathrooms, living rooms, and bedrooms in these types of basements feature one or more walls which are partly or entirely below the grade. An advantage of habitable basements is that heating and cooling costs may be reduced owing to earth sheltering. However, proper moisture control of habitable basements is essential to reduce the risk of moisture damage; this is because high relative humidity (RH) and moisture content (MC) in structures may lead to the growth of mould and rot fungi, structural decay, and reduced thermal performance of the basement envelope [1–4].

The exterior part of the basement envelope is prone to moisture strain owing to high RH from soil/backfill, precipitation/stormwater, and water from snowmelt [5]. These strains are also expected to increase in the near future because climate change entails frequent and intense heavy rainfall and rain-induced floods [6,7]. The moisture strain on a basement envelope may also increase owing to a stormwater management strategy that involves the infiltration of surface runoff into the ground surrounding the building [8]. Even after renovation, older structures may be prone to moisture uptake from the ground owing to poor drainage underneath the foundations. Bathrooms and laundry rooms are commonly placed in habitable basements; this results in a significant indoor moisture supply and a limited ability for the structure to dry inward. In new buildings, site-casts or concrete-block basement walls contain a significant amount of built-in moisture after construction and require structural drying [9].

* Corresponding author.
E-mail address: silje.asphaug@sintef.no (S.K. Asphaug).

https://doi.org/10.1016/j.buildenv.2022.109393
Received 14 May 2022; Received in revised form 6 July 2022; Accepted 10 July 2022
Available online 14 July 2022

Based on existing literature and recommendations, it is possible to build habitable basements with a relatively low risk of moisture damage; this can be achieved by ensuring optimal drainage of walls and floors, insulation on the outside, and protection against water penetration from the outside by using capillary-breaking layers [5]. Vapour-permeable thermal insulation can also be used to enhance the outward drying of basement walls. However, the effect of outward drying on the moisture performance of interior wall parts requires further investigation [10,11].

1.2. Design for outward drying

Several products have been designed to ensure the optimal moisture performance of basement walls, such as dimpled membranes, matrix panels, insulation drainage panels, drainage mats, and spray-on waterproofing membranes. Some products are capable of providing several functions on their own, others are used in combination with other products. For example, various products have been designed to eliminate the need for granular backfill, others are designed to enable outward drying [12]. Outward drying may be particularly beneficial in the following cases: 1) poor drainage below foundations that dampens the rehabilitated walls; 2) a bathroom/laundry room that inhibits inward drying; 3) cases in which the use of organic materials, such as wood, need to be increased to reduce the carbon footprint of the building.

In many countries with cold climates, vapour-permeable thermal insulation is applied to the exterior side of basement walls to realise below-grade outward drying; this is widely practised in Sweden [13], Denmark [14] and Norway [15]. The aforementioned insulation method differs from the conventional strategies (e.g. Canada [16,17], Estonia [18], USA [19] and Finland [20]), in which the exterior side of the walls is protected by a waterproofing membrane, treated with sprays or roll-on compounds, or a dimpled membrane is positioned between the wall and exterior thermal insulation.

The principal theory behind the use of below-grade vapour-permeable thermal insulation is that in heated buildings in cold climates, the temperature (T) across the basement wall decreases from the warm interior side to the cold exterior side. Therefore, vapour from the structure may diffuse through the vapour-permeable thermal insulation, owing to the difference in vapour pressure induced by the temperature differences. Subsequently, the vapour is condensed at the exterior cold side of the exterior insulation/exterior membrane/geotextile and drained to the ground below the building [21]. To mitigate the vapour diffusion, mineral wool boards or expanded polystyrene (EPS) of special qualities can be used. Different products are used with or without a draining backfill, protective exterior membrane, or geotextile. The use of vapour-permeable thermal insulation requires efficient stormwater management and on-site drainage because the exterior side of the structure becomes wet quickly when exposed to liquid water [12].

In Norway, the recommendations for below-grade walls prescribe vapour-permeable thermal insulation with a water vapour diffusion resistance factor of less than 10 to increase outward drying [15]. Moreover, it is recommended that a dimpled membrane should be placed on the outer side of the exterior insulation (exterior position). The latter differs from the recommendations in other cold-climate countries, which prescribe a dimpled membrane to be placed between the concrete and exterior insulation (medial position) or the use of a geotextile as the outer layer when the vapour-permeable thermal insulation is primarily used for drying purposes [5,12]. The dimpled membranes/sheets are designed to provide capillary breaks and vertical drainage. As shown in Fig. 1, a dimpled membrane typically consists of polypropylene sheets with a thickness of 1 mm and approximately 7–10 mm dimples extruded on one side to create an air gap.

The position of dimpled membranes is a subject of discussion among Norwegian building researchers. Those in favour of the exterior placement of the dimpled membranes argue that both solutions can realise robust structures. In contrast, some argue that the effect of outward drying is minimal and inadequately documented, and the air gap behind a dimpled membrane positioned directly on the wall (medial position) can ensure sufficient drying if the air gap is slightly ventilated [22].

1.3. Previous literature

Previous studies have investigated the efficacy of outward drying of basement walls using vapour-permeable thermal insulation. The hygrothermal simulations performed by Geving et al. [11] demonstrated that walls fitted with vapour-permeable thermal insulation ($\mu = 4.4$) exhibit faster drying and lower moisture content (MC) at equilibrium compared with standard EPS ($\mu = 50$). However, the simulations did not consider a dimpled membrane on the exterior side of the insulation. Geving et al. [11] also performed field measurements of desiccation of two basement walls rehabilitated with exterior vapour-permeable thermal insulation on the exterior side. The field measurements did not reveal any signs of drying over a period of 19 months. Blom [23] conducted field measurements of the outward drying behaviour of six concrete basement test walls and measured the temperature, RH, and MC of the wall assemblies. The study did not detect any increased drying effect in the walls with exterior vapour-permeable thermal insulation and exterior dimpled membrane compared with the walls with the dimpled membrane positioned directly on them (between the wall and insulation). The use of vapour-permeable thermal insulation combined with landscape fabric (geotextile) instead of a dimpled membrane and backfill of existing soil is a common approach applied in Sweden [12].

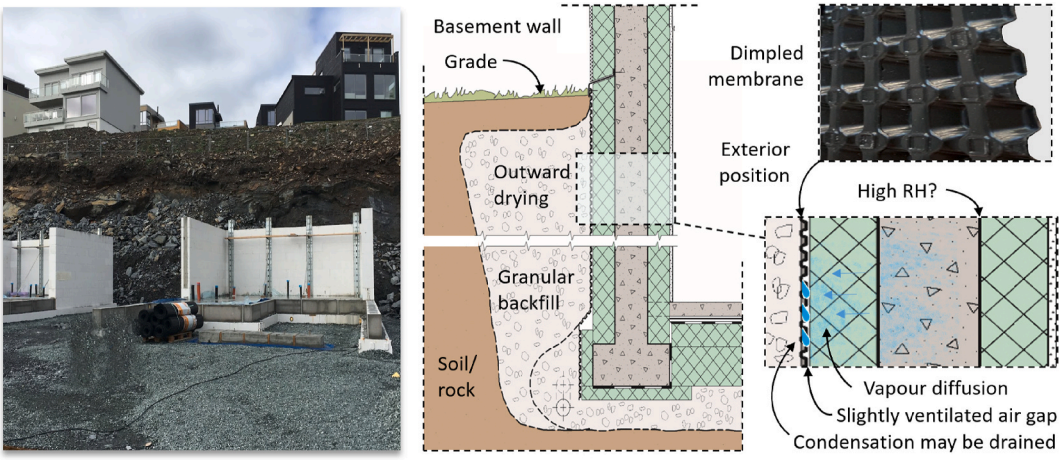

Fig. 1. Basement in dwelling during construction (left). Illustration of basement wall, a dimpled membrane, and a slightly ventilated air gap.

Pallin [12] used hygrothermal simulations to investigate the efficacy of outward drying of concrete basement walls retrofitted with exterior vapour-permeable thermal insulation in the climate of Gothenburg, Sweden. Based on the results, it was reported that the outward drying was slow, and only approximately 6–8 kg/m^2 of the moisture in the wall could be eliminated annually, at maximum. If any of the rain loads that directly hit the ground or drain from the upper wall surfaces accidently penetrate the drainage/insulation board, the expected drying potential can be equalised or reversed. To ensure a positive drying potential, Pallin [12] suggested replacing the landscape fabric with a water vapour barrier.

Few studies have focused on the ventilation and outward drying through the air gap of dimpled membranes used on the exterior side of the basement walls. However, some existing studies have investigated the exterior air gaps in above-grade walls. Although the scope of the following studies is different than that of the present study, their results are nonetheless relevant. Straube [24] performed a laboratory experiment to investigate the role of small gaps in ventilation drying and the optimum gap size required to ensure drainage. According to the results, ventilation drying could play a role in small gaps of approximately 1 mm at a pressure difference of only 1 Pa. Straube and Smegal [25] investigated the role of small gaps in ventilation drying further and used one-dimensional simulation models with source and sink enhancements to simulate the hygrothermal performance of wall systems with drained and ventilated air gaps; this study illustrated the challenges of modelling the real moisture storage of the air in the air gap and the moisture retained on the drainage gap surfaces, highlighting the significance of laboratory investigations and field studies. Finch and Straube [26] investigated the drying of ventilated claddings in above-grade exterior walls. According to Finch and Straube [26], the probable range of ventilation rates depends on the cladding type, cavity dimensions, and venting arrangement and is determined by the thermal and moisture buoyancy and wind pressures. The vent openings are critical details that should be as large as possible and unobstructed. Straube et al. [27] performed field studies on wooden-framed wall systems clad with bricks or vinyl siding. They observed that the drying rates varied significantly under different weather conditions, and the ventilation increased the drying potential of some walls. Furthermore, solar-driven vapour diffusion redistributed the vapour from within the wall to the interior (where it caused damage). Moreover, the ventilation reduced the magnitude of the flow. Rahiminejad and Khovalyg [28] reviewed the ventilation rates in the air gaps behind the cladding of above-grade walls and reported that the stack effect and wind effect are two major mechanisms driving the airflow in ventilated air spaces. Considering basement walls, solar radiation may be more influential on the part of the wall above the grade [12]. Similarly, the wind effect may be more significant on the part above grade than the part below grade; however, the stack effect may be the most significant owing to the temperature difference between the top and bottom of the walls.

Note that various studies have focused on thermally insulated basements. Saber et al. [29] showed that the air gaps in basement walls can be utilised to improve thermal performance. Goldberg and Harmon [30] conducted a comprehensive, large-scale experiment to investigate the moisture durability of interior insulation solutions for basement walls located in cold climates. Straube [9] investigated interior insulation systems by performing both in-situ measurements and hygrothermal simulations. Fedorik et al. [31] investigated various refurbishment strategies for basement walls through hygrothermal simulations, and Blom and Holøs [32] measured the drying behaviour of internally insulated basement walls. However, these studies primarily focused on the performance of the interior insulation systems. They did not address the drying behaviour achieved using exterior vapour-permeable thermal insulation or the positioning of the dimpled membranes. Presently, dimpled membranes are placed at both the exterior and medial positions in practice, as both the configurations can ensure a low risk of moisture failure [15]. However, many basement envelopes still experience extensive failure owing to flawed construction, and knowledge pertaining to robust structures is necessary [30,33]. Further knowledge of the drying ability of basement structures and possible improvements is crucial for the development of more resilient solutions.

1.4. Objective and scope

A laboratory experiment was performed to investigate the drying behaviour of concrete basement walls further and generate data for the validation of hygrothermal simulations [10]. Three concrete wall segments were fitted with different thermal insulations, and different positions of the dimpled membrane were adopted. The wall segments were subjected to steady interior and exterior climates in a climate simulator. The weights of the segments, precipitated condensation, and temperature data were monitored for six months. Although the weights of the walls varied non-uniformly at the beginning, they decreased uniformly during the last four months; they exhibited the same weight loss rate, variations, and total weight change. This indicates that the effect of the thermal insulation and position of the dimpled membrane on outward drying was negligible for the tested concrete quality, even though the MC of the concrete was maximised and the temperature difference across the insulation (driving potential for diffusion) was large (no interior insulation). The results demonstrated the need to further investigate the effect of the concrete quality on the drying behaviour of basement walls and the effect of the air gap behind the dimpled membranes when it is slightly ventilated. The following research questions were raised to address these general inquiries:

1. How do the concrete quality and vapour permeability of exterior thermal insulation affect the outward drying of concrete basement walls?
2. How does the air gap behind a dimpled membrane effect the outward drying of the concrete basement walls?
3. What is the potential of outward drying to improve the moisture performance of thermally insulated concrete basement walls?

Answers to the aforementioned research questions were sought primarily through numerical simulations using the software WUFI®Pro [34] and COMSOL Multiphysics® [35] (henceforth referred to as WUFI and COMSOL). However, this study has the following limitations.

- This study focused on newly built, functionally airtight, and externally drained basement walls above the groundwater table.
- This study focused on walls in basements used for habitation. Unheated or industrial basements were not considered in this study.
- Changes in material properties due to chemical processes, such as curing, were not considered in the simulations.

2. Methodology

2.1. General approach

Simulating the outward drying of thermally insulated basement walls numerically is a complex process requiring at least two dimensions to include the height of the wall [9,36]. In particular, it is challenging to numerically replicate the air exchange in the air gap behind the dimpled membrane and the drainage of condensed moisture. In a coupled heat and moisture transfer model, the dimpled membrane, and the air gap behind it can either be simplified as a homogeneous layer or neglected outright. If a homogeneous layer is included, moisture drying from the concrete accumulates in the thermal insulation and cannot escape through the condensation drainage. In contrast, if the membrane is neglected, moisture diffuses directly to the exterior boundary condition, which may create unrealistically high drying rates.

A better option is to use a coupled heat, air, and moisture model;

however, this approach introduces many complex uncertainties and incurs high computational costs when the full height of the wall (above and below grade) is included. Furthermore, the long-term simulations of basement walls are rendered complex by the below-grade boundary conditions. The boundary conditions vary seasonally and along the depth of the wall, including the possibility of soil freezing during winter. Therefore, a form of simplification is required for comprehensive numerical simulations. This study was conducted in three steps. The purpose of the first two steps was to examine the effect of the dimpled membrane on the outward drying of concrete walls and obtain input and knowledge for the third and final step, which was a full-scale long-term simulation of a basement wall.

The first and second steps were based on the study by Asphaug et al. [10], in which a laboratory experiment was conducted to investigate the outward drying of concrete basement walls and generate data to validate the hygrothermal simulations. Three concrete wall segments with different configurations of thermal insulation and dimpled membranes on the exterior surface were weighed continuously for six months. The wall segments were sealed against moisture transfer by applying epoxy paint on all sides except the exterior surface (which was allowed to dry on the exterior side). In addition, the wall segments were insulated around the perimeter, mounted in a wooden frame, and subjected to a stable cold and humid exterior climate and warm interior climate in a climate simulator, as shown in Fig. 2.

In the first step, the outward drying of the concrete wall segments was investigated using one-dimensional simulation models. In the second step, more advanced two-dimensional airflow models were established to investigate the air exchange in the air gap behind the dimpled membrane further. In the third and final steps, the effect of the outward drying of the concrete on the overall long-term moisture performance of basement walls were investigated. Based on the knowledge gained from the first and second steps, the dimpled membrane was omitted in the third step. The three steps are illustrated in Fig. 3 and described in more detail in Sections 2.2, 2.3, and 2.4.

2.2. Main simulation variables

The main material properties, boundary conditions, and initial conditions used in Steps 1–3 are illustrated in Fig. 3, and a detailed description is provided in Appendix A. Vapour-permeable thermal insulation $\mu > 10$ was adopted in accordance with the Norwegian building design guidelines [15]. To investigate the effect of vapour permeability on outward drying, three types of EPS with different water vapour resistance factors were compared:

- Vapour-permeable EPS $\mu = 4.4$ (applied by Ref. [11]).
- Vapour-permeable EPS $\mu = 8.2$ (measured in the laboratory experiment in question [10]).
- Semi-permeable EPS $\mu = 27.9$ (measured in the laboratory study in question [10]).

Furthermore, three types of concrete obtained from the WUFI software were compared:

- C35/45, high $D_{ww} = 1E\text{-}07$ m^2/s at 100% RH, high vapour resistance ($\mu = 248$).
- Waterproof, medium $D_{ww} = 1.3E\text{-}10$ m^2/s at 100% RH, medium vapour resistance ($\mu = 180$).
- Masea, low $D_{ww} = 5E\text{-}16$ m^2/s at 100% RH, low vapour resistance ($\mu = 76$).

The initial RH of the concrete in the basement wall of Ex. 1 was set to 99% (~100%) because concrete in such systems is cast directly in the formwork of EPS. The concrete in Ex. 2 was simulated using the same initial MC as that in Ex. 1 for comparison.

The size of the air gap openings of the dimpled membrane in Step 2 was difficult to estimate. For comparison, the openings were assumed to be equal at the two positions of the dimpled membrane. As the air gap was assumed to be slightly ventilated, the upper air gap opening was set to 1 mm to enable slight air transfer. The lower air gap opening was varied from 5 mm (the width of the air gap in the simulation model) to a minimum of 1 mm in the simulations.

2.3. Runtime and convergence

Large and complex numerical models require more resources to run efficiently and a well-composed numerical setup to ease convergence. The one-dimensional simulations in Step 1 were performed without convergence failures. However, the two-dimensional air flow simulations in Step 2 were more problematic, especially as the height of the wall increased and the air gap openings reduced. Sufficient convergence and runtime were achieved by removing the several unnecessary details and improving the mesh refinement around the air gap openings. In the long-term simulations in Step 3, implementing the boundary conditions was challenging because the climate varied with the height of the wall, and the climate data consisted of hourly values. Animation was created from the T, RH, and MC plots to analyse the results. An area on the exterior side of the exterior insulation, at the border between above and below grade, was identify as the main cause of errors. Acceptable convergences and runtimes were achieved by 1) reducing the number of data points in the climate files, 2) using an interpolated graph to implement the climate data for one year and repeating it with a modfunction at each boundary, and 3) using a piecewise interpolation of

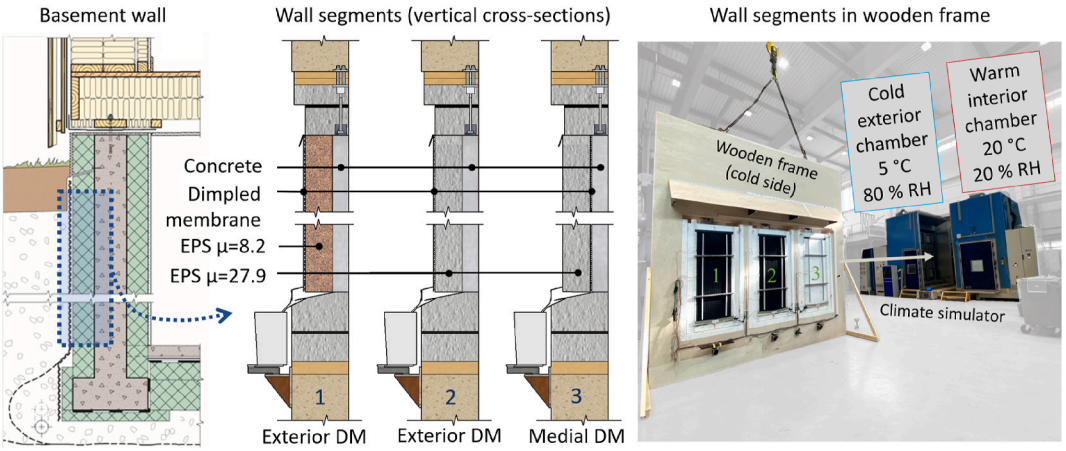

Fig. 2. Concrete wall segments (left) positioned in the wooden frame in the climate simulator (right).

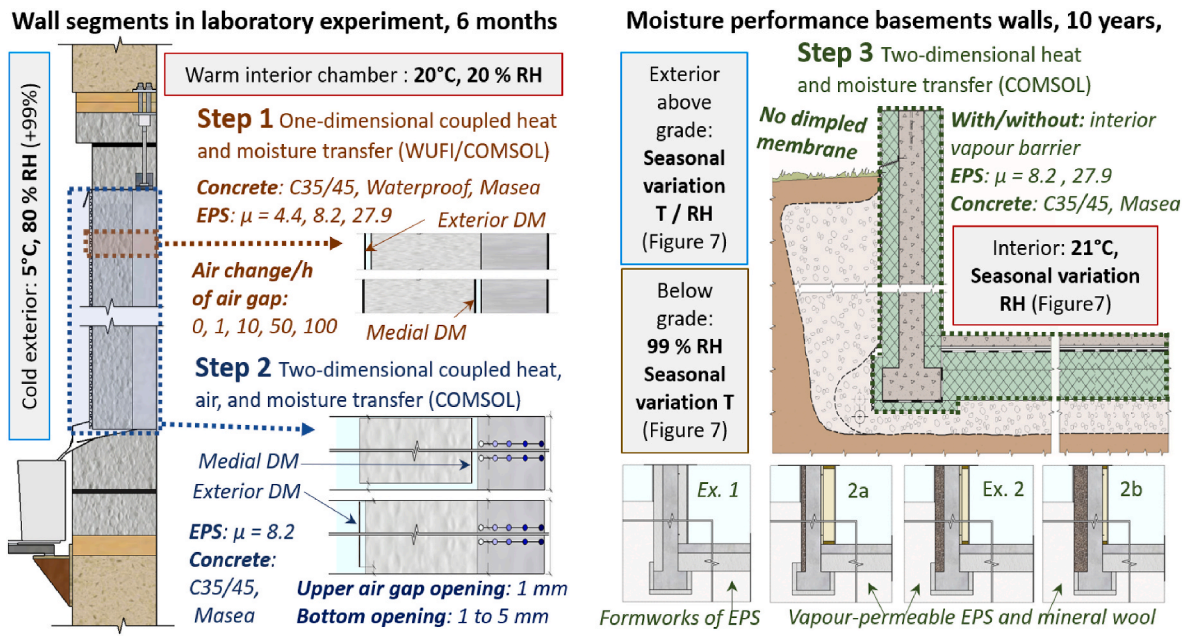

Fig. 3. Main setup, boundary conditions, variable material properties, and model/geometry in Step 1 (upper left), Step 2 (lower left), and Step 3 (right). Detailed descriptions can be found in Section 2.2, 2.3, 2.4, and in Appendix A. Steps 1 and 2 were conducted to investigate the effect of the dimpled membrane on the outward drying in the laboratory experiment. Step 3 was conducted on basement walls without a dimpled membrane, and the effect of outward drying on the moisture performance of interior wall parts was evaluated.

the material data instead of linear interpolation, which reduced the calculation time by half.

2.4. Step 1 - Outward drying of concrete wall segments

The one-dimensional hygrothermal simulations were conducted using WUFI to investigate the influence of vapour permeability of the EPS, concrete characteristics, and position of the dimpled membrane (exterior or medial) on the outward drying of the concrete wall segments.

First, the wall segments were studied by omitting the dimpled membrane from the simulation; it was assumed that the moisture from the concrete could dry directly into the air in the cold and humid climate chamber. Because concrete characteristics may significantly affect the simulated heat and moisture transfer [37] simulations were performed for three concrete types (C35/45, Waterproof, and Masea) and three EPS types (μ = 4.4, 8.33, and 27.9). The simulation period was set to six months in accordance with the laboratory experiment.

Second, the influence of the air exchange behind the dimpled membrane was investigated for both the exterior and medial positions, as illustrated in Fig. 4. Simulations were performed for concrete C35/45, EPS (μ = 8.2), and different air exchanges with exterior air (0, 1,10, 50, and 100). The geometry of the dimpled membrane was simplified, as shown in Fig. 4. Concrete C35/45 was chosen for this investigation because the initial simulations showed that a high liquid permeability would allow for a more rapid initial drying behaviour (faster flattening of the MC graphs). EPS (μ = 8.2) was used to simulate both the exterior and the medial positions. Fig. 4 shows the one-dimensional simulation models, dimensions, boundary conditions, and materials and illustrates the simplification of the dimpled membrane.

2.5. Step 2 - Airflow in air gap behind the dimpled membrane

Step 1 illustrates the need to investigate the effect of the airflow from the exterior into the air gap behind the dimpled membrane on the outward drying of the concrete wall segments.

First, the two-dimensional model of a concrete wall segment was created in COMSOL without an exterior dimpled membrane (one-dimensional layout, concrete, and EPS). The COMSOL model was created according to the procedure described in Ref. [35] and adopted

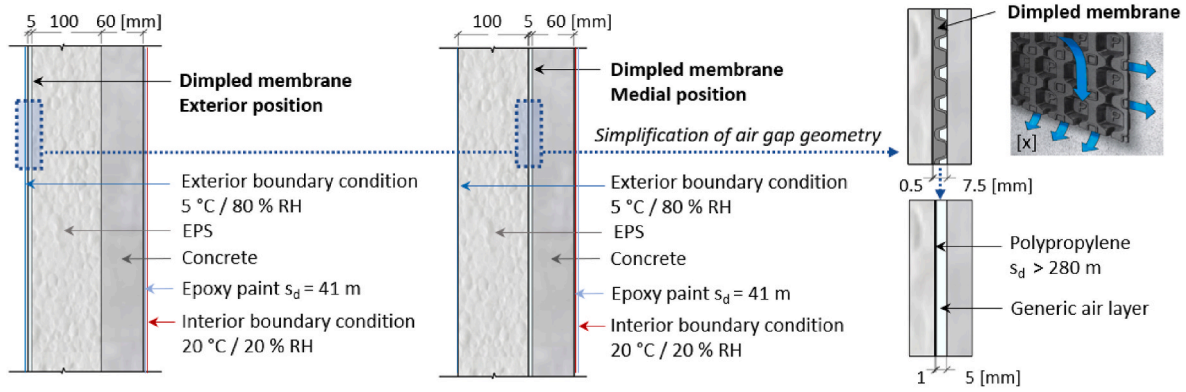

Fig. 4. Step 1 - One-dimensional models of concrete wall segments with exterior and medial position of the dimpled membrane, simplification of air gap geometry, main input data, and dimensions.

the physical principles described in Ref. [38]. The reduction in MC at five depths of the concrete over six months was compared with the MC reduction results obtained using the one-dimensional WUFI model from Step 1 (Appendix B). Neglecting minor deviations, the results can be considered in agreement with each other. Small differences in the liquid transfer coefficient (D_{ww}) in COMSOL and WUFI were identified as the primary causes of the deviation. In COMSOL, D_{ww} was implemented as a function of RH instead of the moisture content. Several points were manually added to the built-in D_{ww} curve of COMSOL to create a more continuous function and achieve a sufficient correlation.

Second, the two-dimensional COMSOL model of the concrete wall segment was developed further to include the dimpled membrane, the air in the exterior climate chamber, and the subsequent air flow within the gap of the dimpled membrane, as illustrated in Fig. 5. The exterior and medial positioning of the dimpled membrane were compared. The height of the concrete was set to 1.5 m, and EPS $\mu = 8.2$ was used. Different thicknesses of the air gap openings (2–5 mm) were investigated. The concrete types C35/45 and Masea were compared.

The model was established according to the procedure described previously [39]. An open boundary was set as the left and upper boundary conditions to include air in the cold exterior chamber, the effect of gravity, and pressure differences. The dimpled membrane was modelled as a *line* and not as a layer to reduce the number of mesh elements and ease convergence. In the moisture transport node, the membrane was defined as a *thin moisture barrier* with a vapour diffusion equivalent air layer thickness (s_d) of 280 m. In the air transfer node, the membrane was defined as an *interior wall* (no slip). In the heat transfer node, the membrane was defined as a *thin layer* (*nonlayered shell)* with thermal resistance (0.0003). Both *laminar flow* and *turbulent flow* were tested; however, *laminar flow* was found to be the most appropriate owing to the low air velocity of the air in the simulations. The air velocity of the air was less than 0.31 m/s within the exterior chamber, less than 0.015 m/s within the air gaps of the medial positioned dimpled membranes and less than 0,025 m/s for the contemporary positioned.

2.6. Step 3 - Long-term moisture performance of basement walls

To investigate the effect of the outward drying of the basement walls on the overall moisture performance of the interior wall parts, long-term simulations of various basement wall-floor transitions were performed. The exterior boundary conditions below the grade included the seasonal variation in temperatures along the height of the below-grade part of the walls. The exterior dimpled membrane was omitted from these assessments to ease convergence, including the air exchange in the air gaps behind the dimpled membrane, which is considered numerically challenging for long-term simulations with varying boundary conditions. Based on the results from Step 2, it can be concluded that the basement walls exhibited a slightly higher drying rate compared to the exterior position owing to the omission of the dimpled membrane.

2.6.1. Numerical model

A two-dimensional model of the basement wall was created using the COMSOL software. The model consisted of a 100 mm thick concrete floor and a 170 mm thick concrete wall. Four configurations with various types of exterior and interior thermal insulation were investigated, as illustrated in Fig. 6. Ex 1. represented a basement wall that is widely used in Nordic countries, with concrete cast directly into formwork of EPS. Ex. 2 represented a basement wall with exterior vapour-permeable thermal insulation and a wooden framework insulated with mineral wool on the interior side. The basement wall in Ex. 2 was also simulated with different thicknesses of the exterior and interior insulation (Ex. 2a and 2b). The two-dimensional models of the concrete basement walls with the main input data, dimensions, and monitoring positions are illustrated in Fig. 6. In normally dry and sufficiently ventilated rooms, omitting the vapour barrier may enable the concrete to dry faster by drying to the interior. In bathrooms, on the other hand, the interior surfaces may have a high vapour resistance, which restricts the ability of the walls to dry inward. The interior surfaces of both basement walls were simulated with and without a vapour barrier.

2.6.2. Exterior boundary conditions above grade

Above the grade, the basement walls were subjected to exterior temperatures and RH variations based on the moisture design reference year (MDRY) of Oslo, Norway (determined by Geving [40] and applied in the WUFI software [34]). The MDRY data were determined based on real measurements; however, the data is composed with higher moisture loads and colder temperatures than in a typical year. The reference year data were based on 3–4 daily measurements, and hourly values were interpolated between them. The original dataset consisted of hourly temperatures and RH values. To reduce the computational costs, a climate file was created using 12-h averages, as shown in Fig. 7. Thus, the number of data points per year was reduced from 8760 to 730. Short- and long-wave radiation and precipitation were neglected.

2.6.3. Interior boundary conditions

The indoor temperature was set at 21 °C. The indoor RH varied with the exterior climate (MDRY Oslo [40]) according to NS ISO 13788:2012 [41] and moisture load according to Humidity Class 3, which is defined in Table 1. The interior boundary conditions are shown in Fig. 7.

2.6.4. Exterior boundary conditions below grade

The below-grade RH was set to 99% according to EN 15026:2007

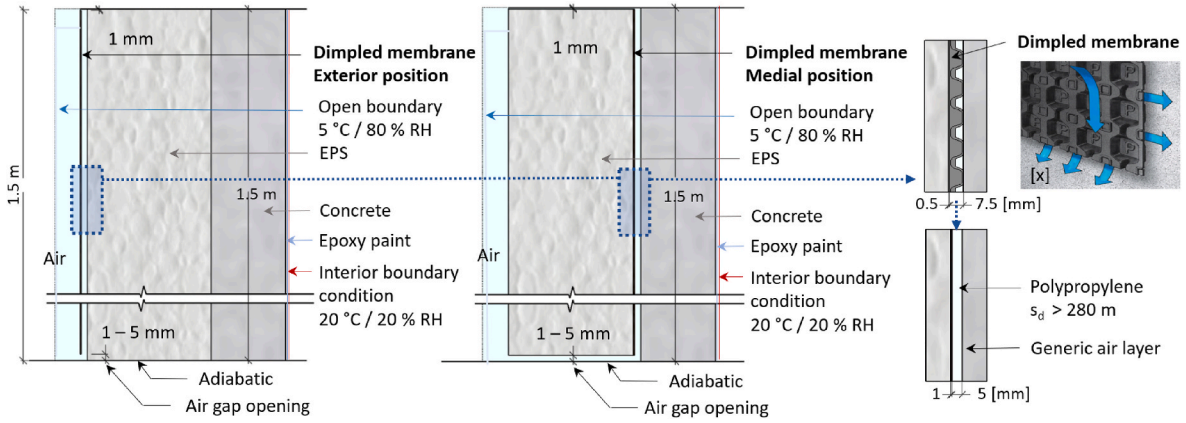

Fig. 5. Step 2 - Two-dimensional models of concrete wall segments with exterior and medial positioning of the dimpled membrane, simplification of the air gap geometry, main input data, and dimensions. Additional simulations were performed to investigate the outward drying changing the RH in the exterior chamber from 80 to 99%, see Fig. C1 Appendix C.

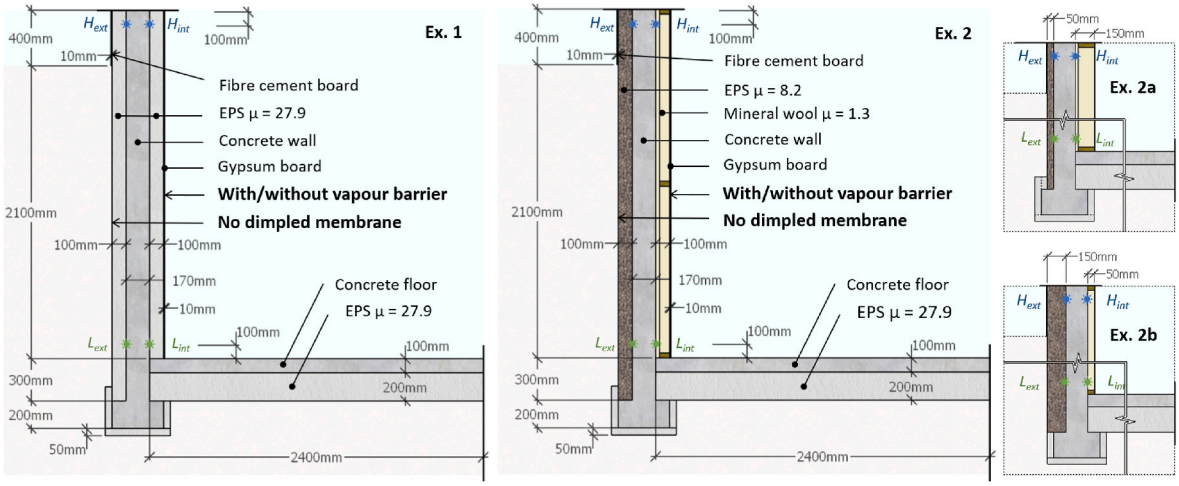

Fig. 6. Step 3 - Two-dimensional models of the concrete basement walls with main input data, dimensions, and monitoring positions. Ex. 1 with formwork of EPS (left) and Ex. 2 with exterior vapour-permeable EPS and interior mineral wool (middle and right). Ex. 1 and Ex. 2 were simulated for two types of concretes without a dimpled membrane on the exterior side and with and without an interior vapour barrier. Simulations were also performed for Ex. 2 for different thicknesses of interior and exterior insulation (left).

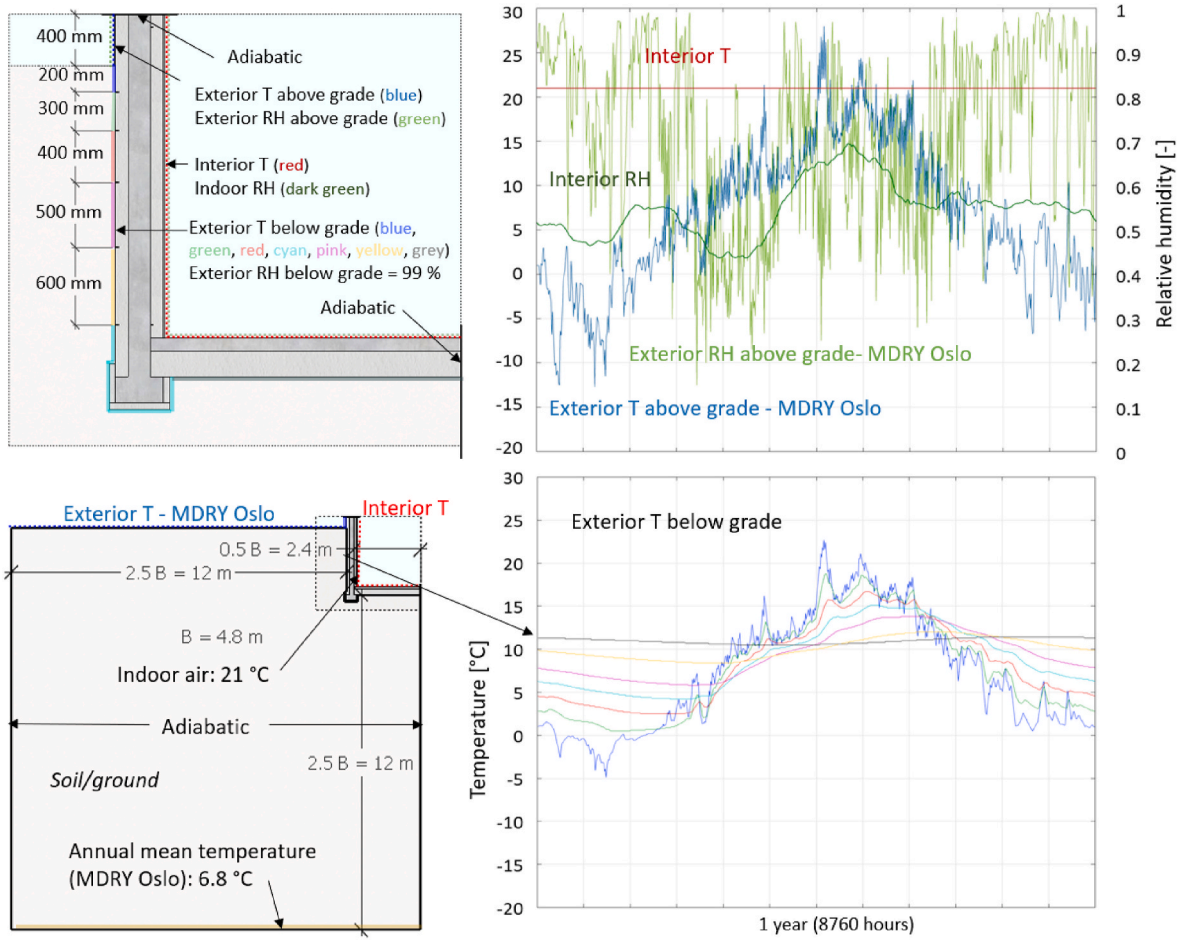

Fig. 7. Main boundary conditions for the basement walls (upper left), temperature and RH variations for the repetitive year (upper right), and varying temperatures below the grade (lower right). Below-grade temperature variations were determined using a separate heat transfer simulation model (lower left). A detailed description of the input parameters is provided in Appendix A.

[42]. The annual temperature variations below the grade were determined using a separate heat transfer simulation of the basement wall-to-floor transition and a large part of the exterior ground. The temperature variations were determined based on the study by Asphaug et al. [36]. Moisture transfer to the soil and evaporation at the soil surface have a significant effect on the heat transfer to the ground [43,

Table 1
Moisture load according to Humidity Class 3.

Outdoor temperature [°C]	−20	0	20	30
Moisture load [g/m^3]	6	6	1	1

44]; however, they were not considered for determining the below-grade boundary conditions. The objective of this study was to compare the moisture performance differences between the different basement walls in a cold climate location. It was assumed that including the additional small variations in the exterior temperature does not significantly affect the relative differences between the walls. The simulation model and main input values are shown in Fig. 7.

The temperature variations on the exterior side of the below-grade basement walls were obtained as integrated averages for each output time at various sections/heights below the grade, as shown in Fig. 7. Initially, the lengths of the sections were equal; however, because the temperature differences between the sections were larger closer to the grade, decreasing the length towards the surface improved the temperature distribution on the basement wall. The indoor air temperature was set to 21 °C, and the lower ground temperature was set to 6.8 °C, which is the annual mean of the MDRY of Oslo. The size of the simulated ground section and soil properties were based on the recommendations of the NS-EN ISO 13793:2001 [45]. A building with dimensions of 12 × 8 m was considered, which resulted in a characteristic width of B = 4.8 m. Freezing was considered by modelling the soil as a phase change material, which changes properties when the temperature approaches −1 °C. The latent heat of fusion of water at 1 atm. was set to 334 kJ/kg, which was the default setting in COMSOL and used by Saaly et al. [46]. The simulation was run for 12 years to stabilise the heat loss. The last year was used for the exterior temperature variations (boundary conditions) below the grade, as shown in Fig. 7. The MDRY of Oslo with 12 h values were used for the exterior air temperature variations. The output times were set to 12 h, which was equal to the dataset used for the wall part above the grade.

3. Results

3.1. Outward drying of concrete wall segments (Step 1)

The one-dimensional coupled heat and moisture transfer simulations of the concrete wall segments were conducted using WUFI. The dimpled membrane was not considered in the initial simulations (Appendix D; Fig. D1). Based on the results, it can be concluded that the concrete characteristics affected the outward drying of the wall segments significantly. The concrete with the highest liquid permeability (C35/45) exhibited the largest weight change. The results elucidated the mechanism of moisture accumulation within the thermal insulation from the C35/45 concrete before the drying of the accumulated moisture by the exterior air. The Masea concrete resulted in little moisture accumulation within the thermal insulation owing to the slow drying of the concrete. Thus, the effect of vapour permeability of the thermal insulation on the outward drying of the concrete may be less for slow-drying concrete.

Subsequently, one-dimensional simulations considering the dimpled membrane were performed using WUFI. The effect of two different positionings of the dimpled membrane (exterior and medial) and that of different air exchange rates at the air gap behind the dimpled membrane were compared (see Appendix D, Fig. D2). The results elucidated the effect of the air exchange with the exterior air on outward drying. When the air exchange with the exterior air was low or absent, the MC of the air in the air gaps increased to 100%; this indicates that condensation would occur within the gaps. When the air exchange was low or absent, the drying of the concrete was larger for the exterior positioning of the dimpled membrane than for the medial positioning. At an air exchange rate of approximately 10, the drying observed for the two positionings was approximately equal.

3.2. Airflow in air gap behind the dimpled membrane (Step 2)

The concrete wall segments with two different positionings of the dimpled membrane (exterior and medial) were compared. For the comparison, different air gap openings at the bottom and different RH of the exterior air were considered (80%, which is according to the laboratory study, and 99%, which is similar to below grade). The results obtained using COMSOL are summarised in Fig. 8 (RH exterior air = 80%). Note that the wall with the medially positioned dimpled membrane enabled the concrete to dry faster at the bottom; however, the wall with an exterior dimpled membrane dried more uniformly along its height. Overall, the walls dried uniformly over six months. However, a difference was observed in the moisture distribution along the height. Note that the MC in the thermal insulation and air gaps increased and decreased during the 6-month period, in accordance with the results from Step 1. Smaller air gap openings increased the RH in the air gaps. Furthermore, it ensured longer periods of condensation. Exterior air with 99% RH resulted in a relatively high MC in the thermal insulation and a slightly slower drying of the concrete segments compared to 80% (Appendix C).

3.3. Long-term moisture performance of basement walls (Step 3)

Long-term simulations of the basement wall-floor transition were performed to investigate the effects of the outward drying of basement walls on the overall moisture performance of the components of the interior wall. Based on the results of Step 2, the exterior dimpled membrane was not considered; thus, the simulations presented slightly higher drying rates than those obtained for the exterior positioning of the dimpled membrane (see Fig. 8). The two basement wall configurations (Ex. 1 and 2) were investigated using the two concrete types (C35/45 and Masea), with and without an interior vapour barrier. The decrease in the RH at the four monitoring points (at the interface between the concrete and insulation) over ten years is shown in Fig. 9.

From the graphs, it can be inferred that the exterior side (dotted lines) of the concrete walls dried faster than the interior side (solid lines) for all the simulated cases. When a vapour barrier was applied to the interior side, the concrete wall in Ex. 2 dried faster than that in Ex. 1 for both types of concrete. The difference was the largest on the exterior side (dotted lines) and the lowest on the interior side (solid green line). At the upper interior side (solid blue line), the RH was affected by the fluctuations in the exterior temperature. Fig. 10 shows the RH and temperature at a cross-section at a high position in the basement walls after 10 years. Ex. 2 was also simulated by varying the thicknesses of the interior and exterior thermal insulation, as shown in Fig. 11. Masea concrete without the interior vapour barrier was selected for the simulations owing to the high interior moisture content portrayed by wall in Ex.2, as shown in Fig. 10.

4. Discussion

4.1. Effect of concrete type and permeability of thermal insulation on outward drying

The outward drying of the concrete wall segments was compared for a period of six months under stable internal (20 °C, 20% RH) and external boundary conditions (5 °C, 80% RH). From the one-dimensional heat and moisture simulations, it was observed that there was a significant difference between the two concrete types, C35/45 and Masea, owing to the differences in material characteristics. As shown in Fig. D1 of Appendix D, C35/45 dried out more than Masea during the six months. The difference between the drying rates decreased as the vapour resistance of the exterior thermal insulation increased. The MC of the cross-sections through the concrete wall segments indicated that the Masea concrete dried the fastest at the surface (owing to the low vapour resistance); however, a slower drying rate was observed deeper

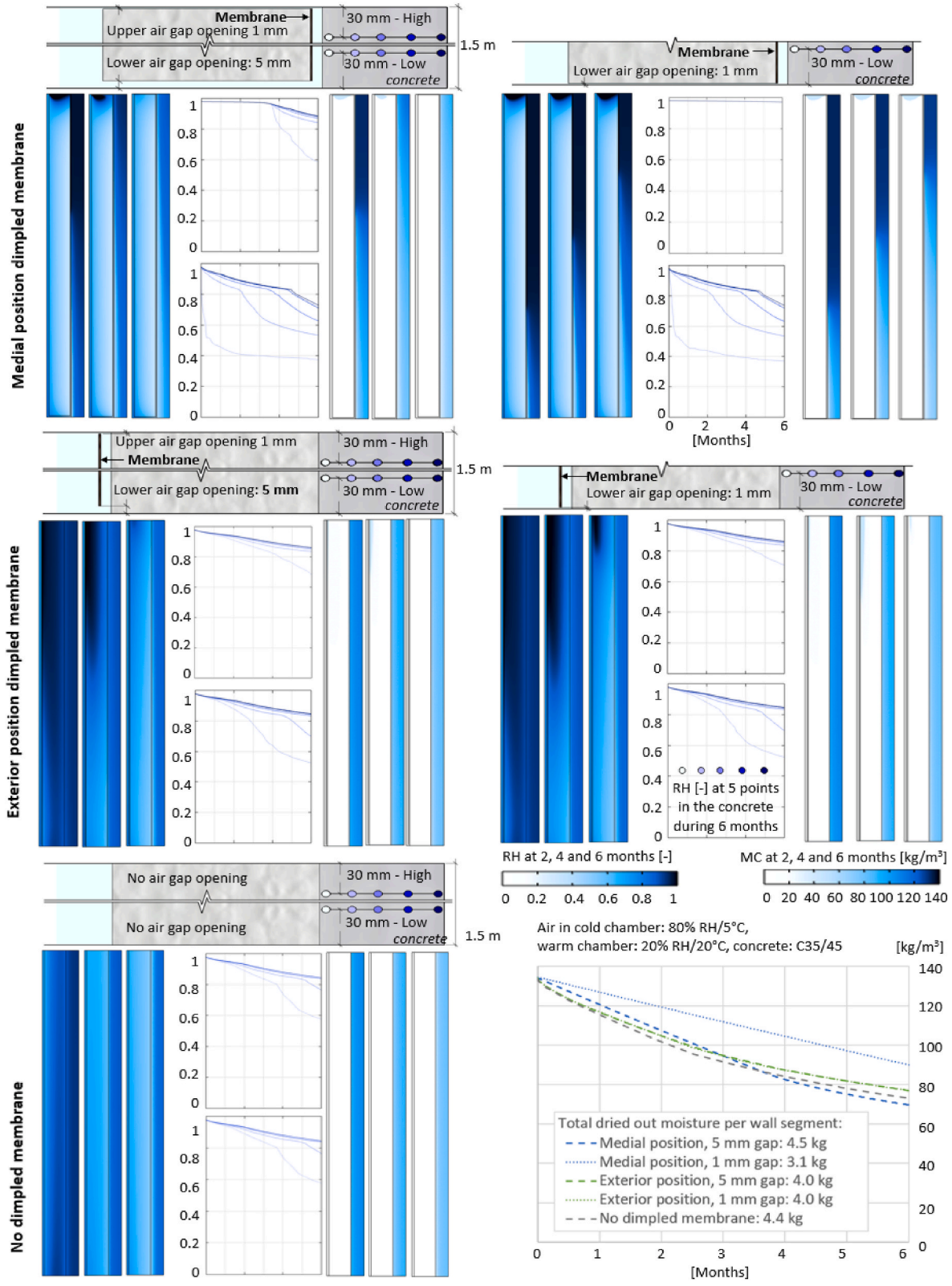

Fig. 8. Concrete wall segments with medial positioning of dimpled membrane and two lower air gap openings (upper left and right), exterior positioning with two air gap openings (middle left and right), and no dimpled membrane (lower left). The upper and lower graphs show the decrease in RH at the five points in the upper and lower part of the concrete, respectively. The left and right plots show the RH and MC for two, four, and six months of drying. The graphs (lower right) show the decrease in average MC of the concrete segments for the five situations considered during six months of drying, and the total amount of dried out moisture per wall segment.

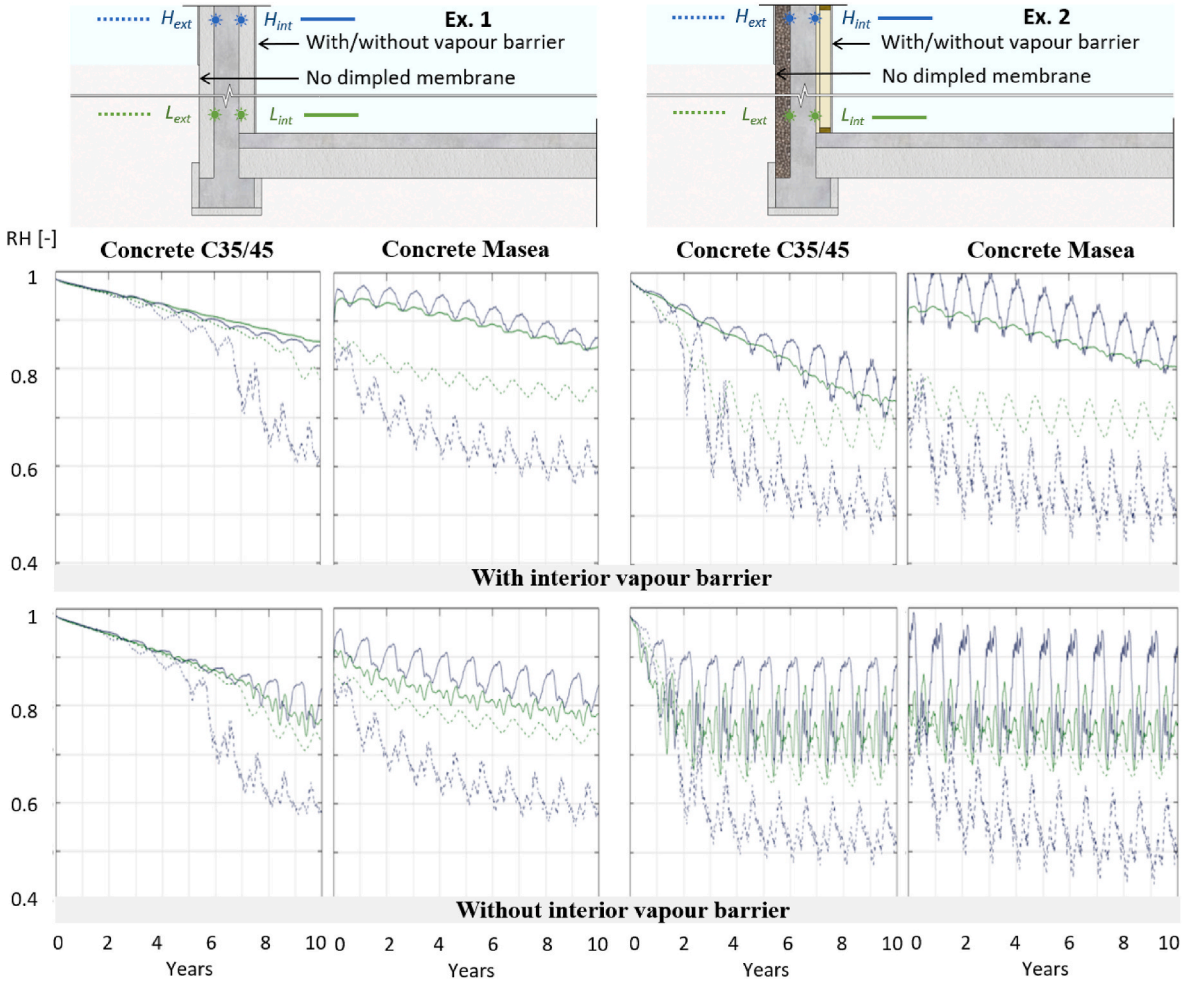

Fig. 9. The ten-years decrease in RH at the four monitoring points located at the interface between the concrete and insulation. Note that the y-axes span from 40% to 100% RH. The positions of the monitoring points are marked in the upper figures.

into the concrete owing to the low liquid conductivity (D_{ww}). The MC at the surface of C35/45 concrete did not decrease as rapidly as that of Masea owing to the high liquid conductivity (D_{ww}) of C35/45; however, the moisture was transferred faster towards the exterior surface from deeper into the concrete. Thus, it can be concluded that C35/45 concrete facilitates more outward drying, at least at high concrete MC. The drying rate of both concretes decreased as the MC decreased because the moisture-dependent liquid transfer coefficient decreased. From Fig. D1 of Appendix D, it can be inferred that the concrete segments insulated with vapour open-thermal insulation ($\mu = 4.4$) dried faster than the uninsulated concrete (which dried directly to the air in the cold and humid climate chamber); this was applicable for all three concrete types; however, the difference was the largest for C35/45 concrete. When the Masea concrete was insulated with the semi-permeable "standard" EPS ($\mu = 27.9$), it dried approximately as quickly as when it was uninsulated.

The drying of the two basement walls over 10 years was investigated, as shown in Figs. 9–11. From the results, it was observed that the Masea concrete dried faster at the surface than deeper into the concrete. C35/45 dried more slowly at the surface compared with the Masea concrete; this is in accordance with the results shown in Fig. D1 in Appendix D. In addition, C35/45 reached a lower MC after 10 years compared with Masea. The fluctuations in the graphs were primarily due to influences from the exterior air temperature. Therefore, the fluctuations were larger in the upper monitoring points than in the lower ones. When it was warmer outside, the moisture was transferred from the exterior to the interior. Note that the oscillations of the RH in the inner monitoring points exhibited a slight delay compared with the oscillations in the outer monitoring points. In addition, the RH in the lower monitoring points fluctuated less than that in the high monitoring points.

4.2. Effect of air gap behind the dimpled membrane on outward drying

The effect of the positioning of the dimpled membrane on the outward drying of the concrete wall segments was compared. The comparisons were made using concrete C35/45 for a period of 6 months under stable warm (20 °C, 20% RH) and cold boundary conditions (5 °C, 80% RH). First, the one-dimensional heat and moisture simulations were performed for different air exchange rates in the air gap, as shown in Fig. D2 of Appendix D. For the exterior positioning of the dimpled membrane, the graphs showed that the moisture in the concrete dried at the same rate, regardless of the air exchange rate behind the dimpled membrane. However, the MC of the generic air layer was unrealistically high in the simulations, suggesting that condensation occurred. For the medial positioning of the dimpled membrane, the concrete dried slowly at low air exchange rates. Note that the results for the medial positioning were similar to the results for the exterior positioning for an air exchange rate of approximately 10/h. However, the air exchange rates are difficult to predict for slightly ventilated air gaps. Concrete C35/45 was used for these assessments. Thus, it can be concluded that concretes that dry slowly, such as Masea, would exhibit smaller differences between the drying rates for the two positionings of the dimpled membrane.

The effect of the airflow through the air gap behind the dimpled membrane on the outward drying of the concrete wall segments was investigated further using two-dimensional heat, air, and moisture

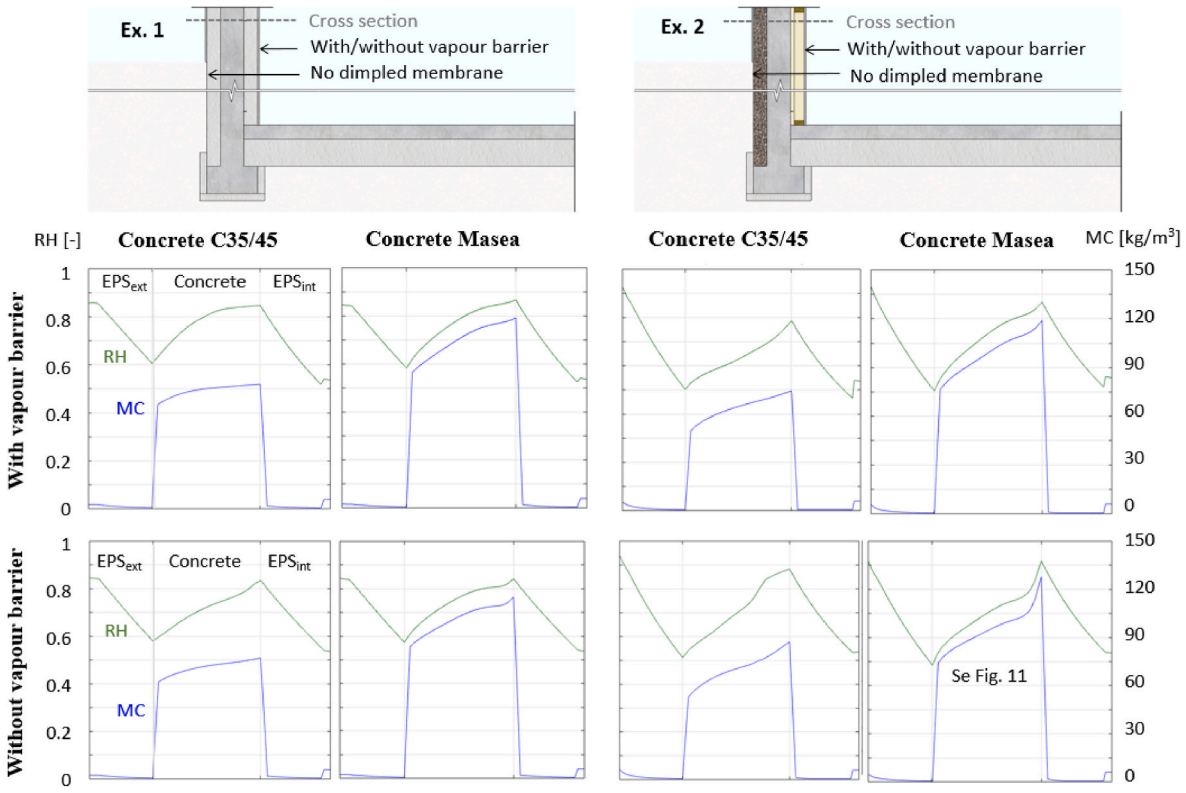

Fig. 10. MC and RH through the cross-section at the high position in the basement walls after 10 years. The position of the cross-section is shown in the upper figures. Ex. 2 with Masea concrete and without an interior vapour barrier is illustrated in Fig. 11 with different thicknesses of the exterior and interior insulation.

simulations, as shown in Fig. 8. From the figures, it can be observed that the concrete wall segments with a medially positioned dimpled membrane dried much faster at the bottom than at the top. However, the segments with an exteriorly positioned dimple membrane dried more uniformly along their height. The concrete wall segments with a medially positioned dimple membrane resulted in relatively slower drying when the bottom air gap opening was reduced from 5 mm to 1 mm. The concrete segments with the exteriorly positioned dimple membranes were less affected by the changes in the opening of the bottom air gap.

The simulations of the wall segments in this study did not consider all the factors that may limit the airflow in and out of the air gaps behind the dimpled membrane in real below-grade basement walls. These factors include the variation in the air gap openings, the density of granular backfilling, wind, and stack effects. Nevertheless, the results obtained are significant as they provide a comparison between the two positionings of the dimpled membrane under similar climate conditions and air gap openings. In addition, the results of the two different positionings of the dimpled membrane were compared with those of the wall segments without a dimpled membrane. The comparison results indicate that applying a dimpled membrane at the exterior positioning, slightly reduced the drying rate, as shown in Fig. 8. For the medial positioning of the dimpled membrane (between the insulation and concrete), it is necessary to ensure that the air gap openings are sufficient to enable drying.

The wall segments in this study were simulated using boundary conditions that reflected the laboratory study. A drawback of the simulation models used in this study is their inability to remove condensed moisture from the air gaps. Instead of being removed, the MC of the air increases to higher levels than the air can realistically hold for a short period. The effect of this uncertainty on the outward drying requires further investigation; however, it was assumed that the outward drying of the concrete segments would be slightly reduced during the condensation period.

4.3. The effect of outward drying on the moisture performance of basement walls

The outward drying of concrete basement walls subjected to varying interior and exterior boundary conditions for over 10 years was investigated, as shown in Figs. 9–11. It was presumed that the walls were protected from exterior liquid water intrusion, either by an exterior dimpled membrane or by other measures, both above and below the grade. Thus, the effect of regular wetting by rain or stormwater was not considered. However, the exterior dimpled membrane was not considered in these simulations, owing to difficulties in including the air flow in the air gap in the full-scale simulation of the basement walls. Outward drying of the concrete wall segments with an exterior positioning of a dimpled membrane was compared with that of walls without a dimpled membrane in Step 2, as shown in Fig. 8; a small difference between the outward drying rates was observed for the two configurations.

Fig. 9 shows the variations in RH at high and low interior and exterior monitoring points at the interface between the concrete and EPS. For the basement wall with EPS formwork (Ex 1), the difference between the drying rate of the two concrete types, both with and without an interior vapour barrier, was small. The Masea concrete dried slightly faster at the exterior monitoring points owing to the low vapour resistance ($\mu = 76$); however, after 10 years, the difference between the drying rate of the two concrete types evened out. The RH at the two interior monitoring points decreased at a relatively steady rate for both the concretes, with and without a vapour barrier; however, the Masea concrete was affected more significantly by the external temperature fluctuations. The basement wall with vapour-permeable exterior insulation and interior wooden frame with mineral wool (Ex 2) exhibited a relatively greater difference between the characteristics of the two concrete types, with and without a vapour barrier. Concrete C35/45 with an interior vapour barrier had a lower interior RH after 10 years compared with the wall with more vapour-resistant EPS in Ex 1. The Masea concrete, which is more vapour-permeable, resulted in higher RH

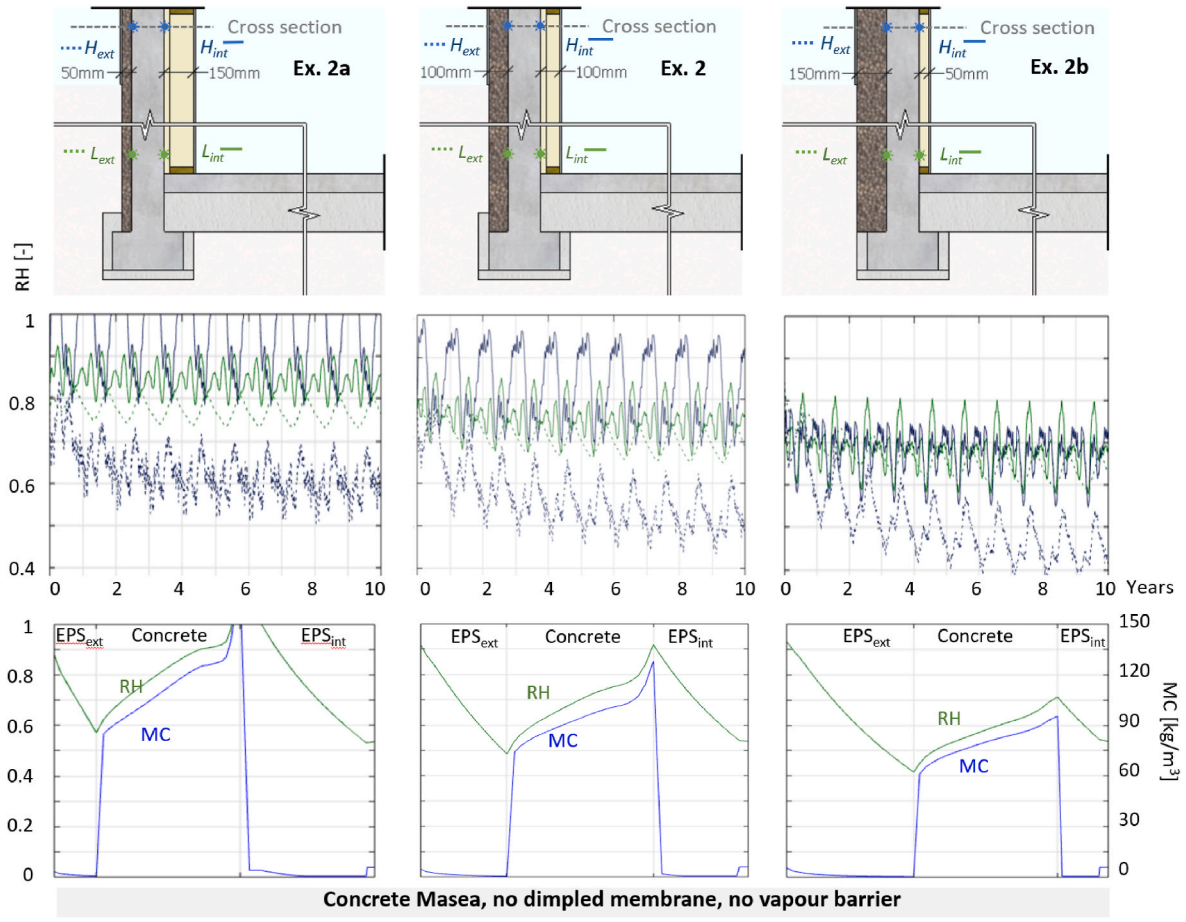

Fig. 11. The 10-year decrease in RH at the four monitoring points (at the interface between the concrete and insulation) (upper). Note that the y-axis spans from 40% to 100% RH. MC and RH through the cross-section at the high position in the basement walls after 10 years (lower). The position of the monitoring points and the cross-section is marked in the upper figures.

on the interior side, even up to 100% in the first years. On the exterior side, however, the RH values were similar. For both the concrete types, the interior vapour barrier resulted in a higher RH on the interior side of the concrete. This indicates that if a vapour barrier is to be used in this type of wall configuration, it should be positioned between the concrete wall and interior insulation.

The basement walls in Exs. 1 and 2 are conventional walls, and they are not considered typical high-risk structures in terms of moisture damage. Note that the objective of investigating the two different types of basement walls was not to determine the wall with the best performance but rather to elucidate the effects of outward drying. Fig. 10 shows that the moisture performance of the basement walls decreased as the thickness of the interior insulation increased. The best performance was achieved when most of the exterior vapour-permeable insulation was positioned on the exterior side.

The primary goal of a moisture-resilient basement wall design is to prevent the walls from being subjected to liquid water from the exterior side. Thus, for externally insulated, well-drained, and airtight basement walls in new buildings with good ventilation, the effect of external drying is considered less significant. For older basement walls, where poor drainage results in moisture absorption via foundations, outward drying may be a suitable method to achieve a drier wall. In this case, the thermal insulation should mainly be positioned on the exterior side of the concrete.

4.4. Uncertainties and limitations

Different concrete characteristics results in different drying rates of the basement walls. The spans of the different properties exhibited by the concrete used in basements requires further investigation.

The initial RH of the concrete in the basement wall of Ex. 1 was set to 99% (~100%) because for this type of basement walls, the concrete is cast in situ in an EPS formwork. For comparison, the concrete in Ex. 2 was simulated using the same initial MC as that in Ex. 1. The concrete used in Ex. 2 might have dried slightly at the surfaces during the time before insulation was added. It was assumed that this drying did not significantly affect the overall results/comparison over 10 years.

In this study, the accuracy of the numerical model in realistically replicating the moisture transfer in the concrete during the drying process was uncertain. The complex coupled heat and moisture transfer models for building components always involve the simplification of real-life factors. Moreover, some materials (e.g. concrete) do not conform to the simplified transport equations, and their material properties are dependent on their present and past moisture content. Therefore, materials with pronounced hysteresis in their moisture storage function (e.g. concrete) may not be accurately described by an averaged moisture storage function [38]. The total moisture transfer resulting from the combination of the liquid and vapour transport processes under varying thermal conditions is also difficult to calculate; this is because the two flows occur simultaneously and cannot be separated for laboratory experiments. The errors caused by these general inaccuracies may be negligible or severe. The results should be compared with measurements to determine the reliability of the calculations.

5. Concluding remarks

The concrete characteristics significantly affected the prediction results of the drying of concrete wall segments. During the six-month period, the concrete with a high liquid transfer coefficient and high vapour resistance (C35/45) dried faster than the concrete with a low liquid transfer coefficient and low vapour permeability (Masea). The Masea concrete dried faster at the exterior surface but exhibited a slow drying rate owing to the low rate of capillary moisture transfer. The concrete with a high liquid transfer coefficient (C35/45) dried slower at the surface but dried faster all the way through the concrete compared with the Masea concrete; thus, it exhibited an overall faster drying rate at high MC. The difference between these two types of concrete also decreased as the vapour resistance of the exterior thermal insulation increased. The concrete insulated exteriorly with vapour-permeable thermal insulation ($\mu = 4.4$) dried faster than the uninsulated concrete, in the laboratory setting (with cold and humid air in the exterior climate chamber, and warm air in the interior climate chamber). This tendency was observed for all three types of concrete; however, the difference was the largest for the concrete with the highest liquid transfer coefficient (C35/45). When the concretes were insulated with the semi-permeable EPS ($\mu = 27.9$), the concrete with the lowest liquid transfer coefficient (Masea) dried approximately as fast as the uninsulated concrete.

The concrete wall segments with a medially positioned dimpled membrane dried much faster at the bottom than at the top, whereas the wall segments with an exteriorly positioned dimple membrane dried uniformly along their height. The concrete wall segments with a medially positioned dimpled membrane exhibited relatively slower drying when the bottom air gap opening was reduced from 5 to 1 mm. The wall segments with exteriorly positioned dimpled membrane was less affected by the changes in the bottom air gap opening; however, more moisture accumulated in the exterior parts of the exterior thermal insulation. The results indicated that the basement walls exhibited a slightly reduced drying rate when the exteriorly positioned dimpled membrane was omitted.

For the basement wall with EPS formwork (Ex. 1), the difference between the drying rate exhibited by the two concretes, with and without an interior vapour barrier, was low. The basement wall with vapour-permeable exterior insulation and an interior wall assembly insulated with mineral wool (Ex. 2) exhibited a relatively greater difference between the characteristics of the two concretes, with and without a vapour barrier. The basement wall with the fastest drying concrete (C35/45) and an interior vapour barrier exhibited a lower interior RH after 10 years compared with the wall with EPS with greater vapour resistance (Ex. 1). In contrast to Ex. 1, the use of Masea concrete resulted in a higher RH on the interior side, even up to 100% in the first year. However, on the exterior side, the RH was similar. For the two types of concrete, the interior vapour barrier resulted in a higher RH on the interior side of the concrete. The results indicate that for optimum performance, the vapour barrier should be positioned between the concrete and interior insulation. However, the span of the moisture properties of conventional concretes used in basement walls needs further investigation.

Therefore, a general conclusion regarding the effects of outward drying on the moisture performance of the insulated basement walls cannot be solely based on the simulations performed in this study. To determine the reliability of the simulations, the results should be compared with measurements of structures subjected to realistic climates. However, the results indicate that placing a dimpled membrane on the exterior side of vapour-permeable thermal insulation can ensure better outward drying. However, the overall effect will depend on the concrete characteristics. If the drying rate of the concrete is low, the effect of vapour-permeable thermal insulation will be less prominent. Positioning the dimpled membrane between the concrete and exterior insulation may be more feasible and can ensure better protection of the concrete and dimpled membrane. In contrast, if the drying rate of the concrete is slow, the aforementioned position of the dimpled membrane may result in sufficient outward drying if the air gap. This position may also increase the drying rate of the lower part of the wall.

CRediT authorship contribution statement

Silje Kathrin Asphaug: Writing – review & editing, Writing – original draft, Visualization, Validation, Software, Project administration, Methodology, Investigation, Formal analysis, Conceptualization. **Erlend Andenæs:** Writing – review & editing. **Stig Geving:** Writing – review & editing, Supervision. **Berit Time:** Writing – review & editing, Supervision, Funding acquisition. **Tore Kvande:** Writing – review & editing, Writing – original draft, Visualization, Supervision, Resources, Methodology, Funding acquisition, Conceptualization.

Declaration of competing interest

The authors declare that they have no known competing financial interests or personal relationships that could have appeared to influence the work reported in this paper.

Data availability

Data will be made available on request.

Acknowledgements

The authors are grateful for the financial support from (1) the Research Council of Norway and several partners through the Centre for Research-based Innovation “Klima 2050” (Grant No 237859) (see www.klima2050.no). We would like to thank Erlend Kristiansen for the input and support in the process of setting up the simulation models in COMSOL.

Appendix

Appendix A. Material properties, boundary conditions and initial conditions

The material properties, initial conditions, and boundary conditions applied in the simulation are listed in Tables A1–5.

Table A1
Hygrothermal properties of the wall segments/basement walls in Steps 1, 2, and 3. The properties of mineral wool and wood were based on data from the COMSOL library. The others were based on data from the WUFI Material database [34].

	Dimpled membrane	Air layer (generic)[a]	EPS, 4.4	EPS, 8.2	EPS, 27.9	Concrete C35/45	Concrete Waterproof	Concrete Masea	Epoxy paint[b]	Gypsum	Vapour barrier	Mineral wool	Wood
Step	1	1	1	1, 2, 3	1, 3	1,2,3	1	1,3	1	3	3	3	3

(*continued on next page*)

Table A1 (*continued*)

	Dimpled membrane	Air layer (generic)[a]	EPS, 4.4	EPS, 8.2	EPS, 27.9	Concrete C35/45	Concrete Waterproof	Concrete Masea	Epoxy paint[b]	Gypsum	Vapour barrier	Mineral wool	Wood
Thickness [mm]		5	100	100	100	60	60	60	1	10	n.a.	100	n.a.
Bulk density [kg/m^3]	130	1.3	26.9	26.9	23.0	2220	2300	2104	130	574	n.a.	73	532
Porosity [m^3/m^3]	0.001	0.999	0.95	0.95	0.95	0.18	0.18	0.22	0.001		n.a.	n.a.	n.a
Thermal conductivity [W/mK]	3	0.047	0.0348	0.0348	0.0348	1.6–2.5	1.6–2.5	1.3–2.2	2.3	Tab. A1	n.a.	0.035	Tab. A2
Specific heat capacity [J/kgK]	1500	1000	1500	1500	1500	850	850	776	2300	1100	n.a.	850	2700
Water vapour diffusion resistance factor [−]	280 000	0.79	4.4	8.33	27.9	248	180	76	41 000	6.9	n.a.	1.4	Tab. A2
s_d-value [m]	280	n.a.	0,44	0.33	2.79	14.88	10.8	4.56	41		10	1e-14	n.a.
Liquid transfer coefficients	n.a.	n.a.	n.a.	n.a.	n.a.	Tab. B6			n.a.	Tab. A2			Tab. A2
Moisture storage function	Tab. A2												

[a] Without additional moisture capacity.
[b] In Step 2, epoxy paint was included in the interior surface transfer coefficient.

Table A2
Moisture storage function of the materials described in Table A1.

DM/Epoxy paint	Air layer	EPS	C35/45	Waterproof	Masea	Gypsum	Mineral wool	Wood
RH:MC	RH:MC	RH:MC 0:0	RH:MC 0:0	RH:MC	RH:MC 0:0	RH:MC	RH:MC	RH: λ
0:0	0:0	0.5:0.461	0.33:37	0:0	0.065:25.5	0:0	0:0	0:0.1
0.5:0.000485	1:0.017	0.6:0.687	0.43:38	0.05:27	0.113:29.6	0.33:5	0.33:0.51	0.97:0.15
0.6:0.000724		0.7:1.06	0.63:65	0.1:32	0.329:46.1	0.75:7	0.75:0.62	1:0.6
0.7:0.00112		0.8:1.79	0.8:75	0.15:34	0.582:80.1	0.97:18	1:4.1	RH:μ
0.8:0.00188		0.85:2.49	0.83:76	0.2:35	0.754:101	1:370		0:200
0.85:0.00262		0.9:3.83	0.93:104	0.3:37	1:144	RH: D_w		0.25:180
0.9:0.00403		0.91:4.26	1:147	0.4:40		0:1.85e-10		0.5:65
0.91:0.00448		0.92:4.78		0.5:48		0.8:1.85e-10		0.6:45
0.92:0.00503		0.93:5.43		0.6:58		1:1.59e-7		0.7:30
0.93:0.00572		0.94:6.27		0.7:72		RH:λ		0.9:20
0.94:0.0066		0.95:7.38		0.8:85		0:0.19		1:10
0.95:0.00777		0.96:8.94		0.9:100		0.97:0.21		RH:WC
0.96:0.00941		0.97:11.3		0.95:118		1:0.6		0:0
0.97:0.0119		0.98:15.1		1:150				0.55:45
0.98:0.0159		0.99:22.7						0.75:80
0.99:0.0239		0.995:30.2						0.97:185
0.995:0.0318		1:44.8						1:870
1:0.0471								RH: D_w
								0: 1.32e-13
								0.65:1.32e-13
								1:8.03e-11

Table A3
Material properties of the soil/ground considered in Step 3. After a comparison between the available sources, the properties provided in NS EN ISO 13793:2001 were used for the simulations.

	NS EN ISO 13793:2001		NS-EN ISO 13370:2017		NS-EN ISO 10456:2007+NA:2010		WUFI
	Homogeneous soil		Clay or silt	Sand or gravel	Clay or silt	Sand or gravel	12 types of soil
	Unfrozen	Frozen					
Bulk density [kg/m^3]	1350	1350	n.a.	n.a.	1200–2200	1700–2200	1267–1579
Thermal conductivity [W/mK]	1.5	2.5	1.5	2	1.5	2.0	Varies with moisture content
Water content [kg/m^3]	450 90% degree of saturation	450 90% degree of saturation	n.a.	n.a.	n.a	n.a	n.a
Heat capasity [J/m^{3}K]	3000000	1900000	3000000	2000000	n.a.	n.a	n.a.
Specific heat capacity [J/kgK]	2222	1407	n.a	n.a.	1670–2500	910–1800	850

Table A4
Boundary conditions used in Steps 1,2, and 3.

Step	Surface	Temperature [°C]	Heat transfer coefficient, α [W/(m²·K)] (Heat resistance [(m²·K)/W])	RH [%]	Water vapour transfer coefficient[1], β_p [kg/m²sPa] or [s/m]
1	Interior	20	8 (0.125) [WUFI]	20	2.2e-8[1] (Epoxy paint in separate layer)
	Exterior	5	17 (0.0588) [WUFI]	80	8e-8[1]
2	Interior	20	8 (0.125) [WUFI]	20	4.9e-12 (ink. Epoxy paint)
	Exterior	5	17 (0.0588) [WUFI]	80/100	8e-8[1]
3	Interior	21	Wall: 8.0 (0.125) [EN 15026:2007] Floor: 5.9 (0.17) [EN 15026:2007]	Fig. 6	2.2e-8[1] 4.1e-8[1]
	Exterior, above grade:	Fig. 6	20 (0.05) (incl. 10 mm fibre cement board)	Fig. 6	3e-10 (incl. 10 mm fibre cement board)
	Exterior, below grade:	Fig. 6	n.a.	99% [EN 15026]	n.a.

[1] Derived from the heat transfer coefficient: $\beta_p = 7{\cdot}10^{-9}\alpha$ [38].

Table A5
Initial conditions used in Steps 1,2, and 3.

Step		Dimpled membrane	Air layer	EPS Mineral wool	Concrete C35/45	Concrete Waterproof	Concrete Masea	Epoxy paint	Wood
1	Temperature [°C]	20	20	20	20	20	20	20	20
	Water content[1] [kg/m³] (RH)	0.002	0.01	(1.79) 0.8	146.39 (0.999), 147 (~1)	149.36 (0.999), 150 (~1)	143.83 (0.999) 144 (~1)	0.002	(0.8)
2	Temperature [°C]	20	20	20	20	20	20	20	20
	Water content[1] [kg/m³] (RH)	0.002	0.01	(1.79) 0.8	134.71 (0.98)	137.2 (0.98)	140.5 (0.98)	0.002	(0.8)
3	Temperature [°C]	21	21	21	21	21	21	21	21
	Water content[1] [kg/m³] (RH)	n.a.	n.a.	(1.79) 0.8	134.71 (0.98)	137.2 (0.98)	140.5 (0.98)	n.a.	(0.8)

The liquid transport coefficient is expressed as a function of the water content in the WUFI and converted to a function of RH for use in COMSOL (see Table A6). Only D_{ww} was active in the simulation because of the absence of rain. In WUFI, moisture storage functions are described by linear interpolation; thus, a linear interpolation was also used in COMSOL in the comparison between COMSOL and WUFI an in Step 2. In Step 3, piecewise cubic interpolation was selected, as it is easier to solve numerically.

[1] The concrete in the laboratory experiment had a high initial MC resulting from curing in a water bath for 28 days after casting. At free saturation, the water content in the concrete corresponded to an RH of approximately 1. This was numerically difficult to solve using COMSOL; thus, RH = 0.999 was used for the initial comparison between the WUFI and COMSOL and in Steps 1. RH = 0.98 was used in Step 2 to ease convergence.

Table A6
Liquid transport coefficients of concrete.

	WUFI Material database			Used in the COMSOL model (Step 2 and 3)		
	wc [kg/m³]	D_{ww} [m²/s] (redistribution)	D_{ws} (wc)[m²/s] (suction)	RH [−]	D_{ww} [m²/s] (redistribution)	D_{ws} (wc)[m²/s] (suction)
C35/45	0	2.00E-11	1.00E-09	0	2.00E-11	1,00E-09
				0.1	2.70E-11	
	29	4.00E-11	4.00E-09	0,2587	4.00E-11	4,00E-09
	72	6.00E-11	1.00E-08	0,749	6.00E-11	1,00E-08
				0.8	8.00E-11	
				0.87	1.90E-10	
	100	4.00E-10	n.a.	0,916	4.00E-10	n.a.
	116	8.00E-10	2.00E-08	0,9496	8.00E-10	2,00E-08
				0.96	2.50E-9	
	130	8.00E-09	3.00E-08	0,9724	9.00E-9	3,00E-08
				0.985	3.00E-8	
	147	1.00E-07	3.00E-07	1	1.00E-07	3,00E-07
Masea	0	0	0	0	0	0
	101	5E-18	1.44E-8	0.754	5E-18	1.44E-8
				0.82	5.1E-18	
				0.85	1E-17	
				0.9	5E-17	
				0.95	2E-16	
	144	5E-16	2.86E-8	1	5E-16	2.86E-8
Waterproof	0	0	0	n.a		
	72	7.4E-12	7.4E-11			
	85	2.5E-11	2.5E-10			
	100	1E-10	1E-9			
	118	1.3E-10	1.2E-9			

Appendix B. Comparison between COMSOL and WUFI

A two-dimensional model of the concrete wall segment from Ref. [10] was created using one-dimensional heat and moisture transfer physics in COMSOL. The geometry and user-controlled mesh called "Mapped" (rectangular mesh) are shown in Fig. B1. The epoxy paint on the interior side was modelled as a generic layer of 1 mm. A one-dimensional model of the same concrete wall segment was created in the WUFI. The grid was an Automatic (II) Fine 100 grid. In WUFI, the increased accuracy and adapted convergence were selected, and the adaptive time step control was enabled with step and max. stages: 5. The number of convergence failures was controlled; it was 0 for all simulations. The reduction in the MC at five concrete depths over six months was compared. The first comparisons showed large deviations between the results of the two programs. Corrections were made for both models to reduce the differences. Some of the changes were as follows:

- The material data input was improved.
- The transfer coefficients were improved.
- The errors in the input data were corrected.
- The mesh in the COMSOL model was improved.

Small differences in the liquid transfer coefficient D_w between the two programs were identified as the primary cause of the deviation. The small differences in D_w were attributed to the implementation of the COMSOL as a function of RH instead of MC. Several points were added to "smooth" the D_w -graph until sufficient correlation between the two programs was achieved. The reduction in MC at the five concrete depths over six months is shown in Fig. B1.

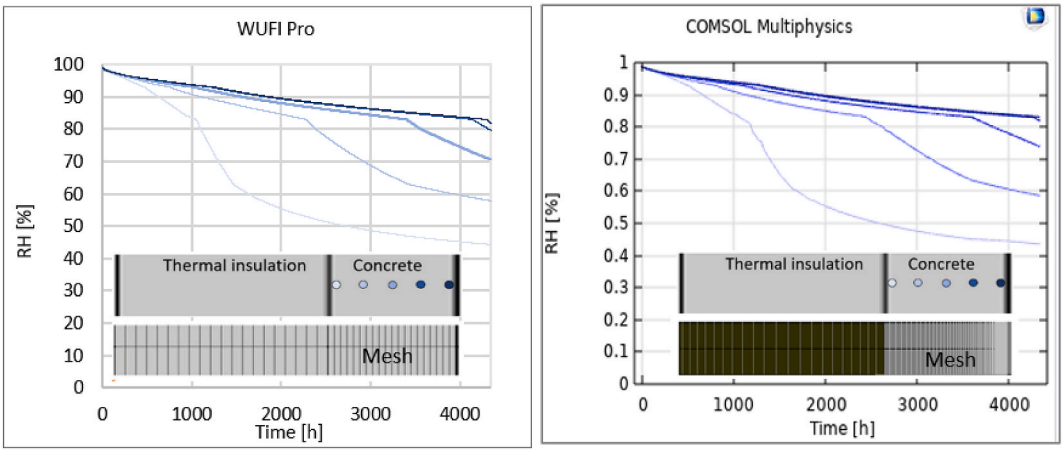

Fig. B1. The simulation models, mesh, and decrease in RH at five points in the concrete during a period of six months obtained using WUFI (left) and COMSOL (right).

Appendix C. Impact of RH in the cold humid climate chamber in Step 2

The RH in the exterior climate chamber in the laboratory experiment was intended to be ~100%; however, owing to the freezing of the cooling pipes, maintaining a low temperature of approximately 5 °C proved to be difficult. Therefore, several tests were conducted, and a temperature of 5 °C and 80% RH was maintained by defreezing for 30 min each day. Figure C1 shows the comparison between the outward drying of the wall segments in the laboratory with 80% RH and outward drying of the wall segments in the exterior climate chamber with 99% RH.

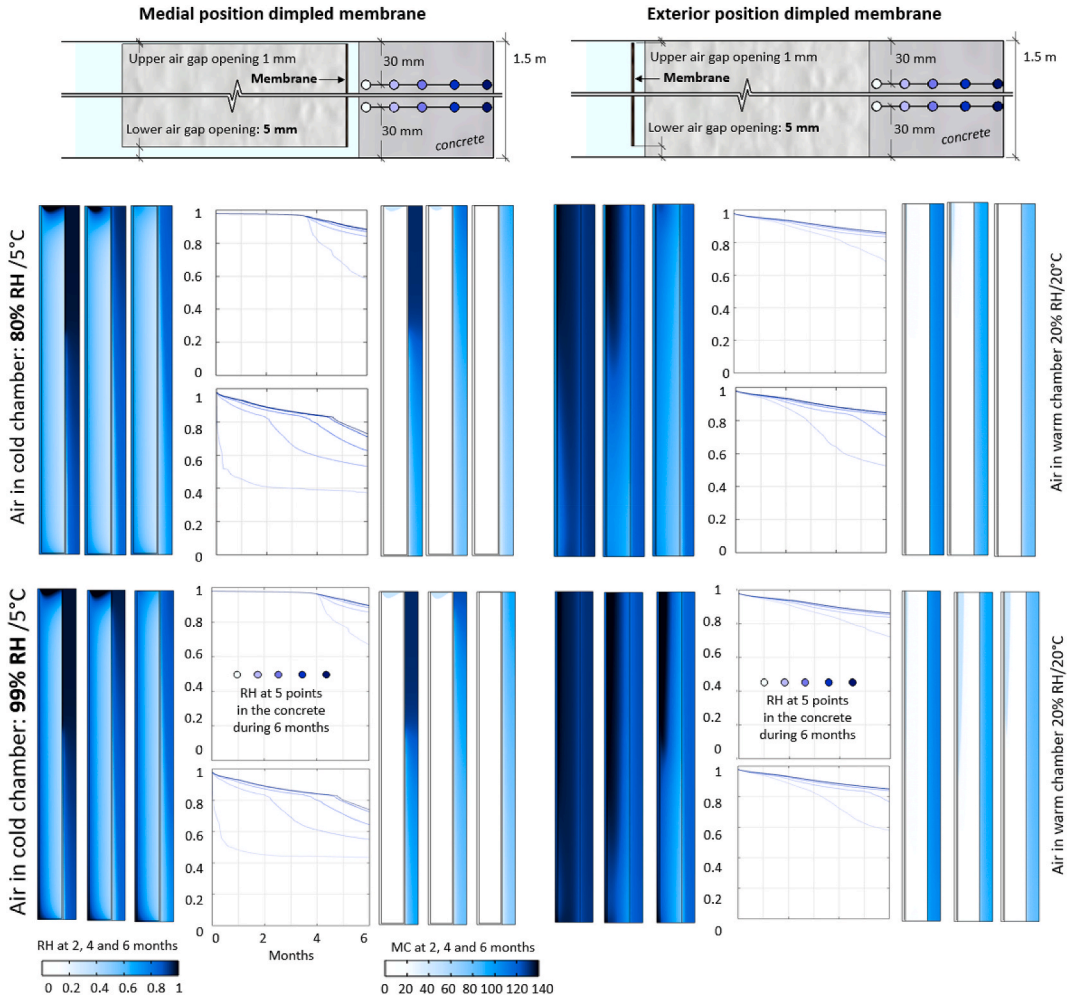

Fig. C1. Drying of the concrete wall segments in the laboratory experiment with 80% RH in the exterior cold and humid climate chamber (upper); drying of the wall segments in the exterior climate chamber with 99% RH (lower). Concrete wall segments with medial positioning (left) and exterior positioning (right) of the dimpled membrane. The upper and lower graphs in each illustration show the decrease in RH during six months of drying at the five points in the upper and lower part of the concrete, respectively. The left and right plots show the RH and MC at two, four, and six months of drying.

Appendix D. Results from one-dimensional simulations in Step 1

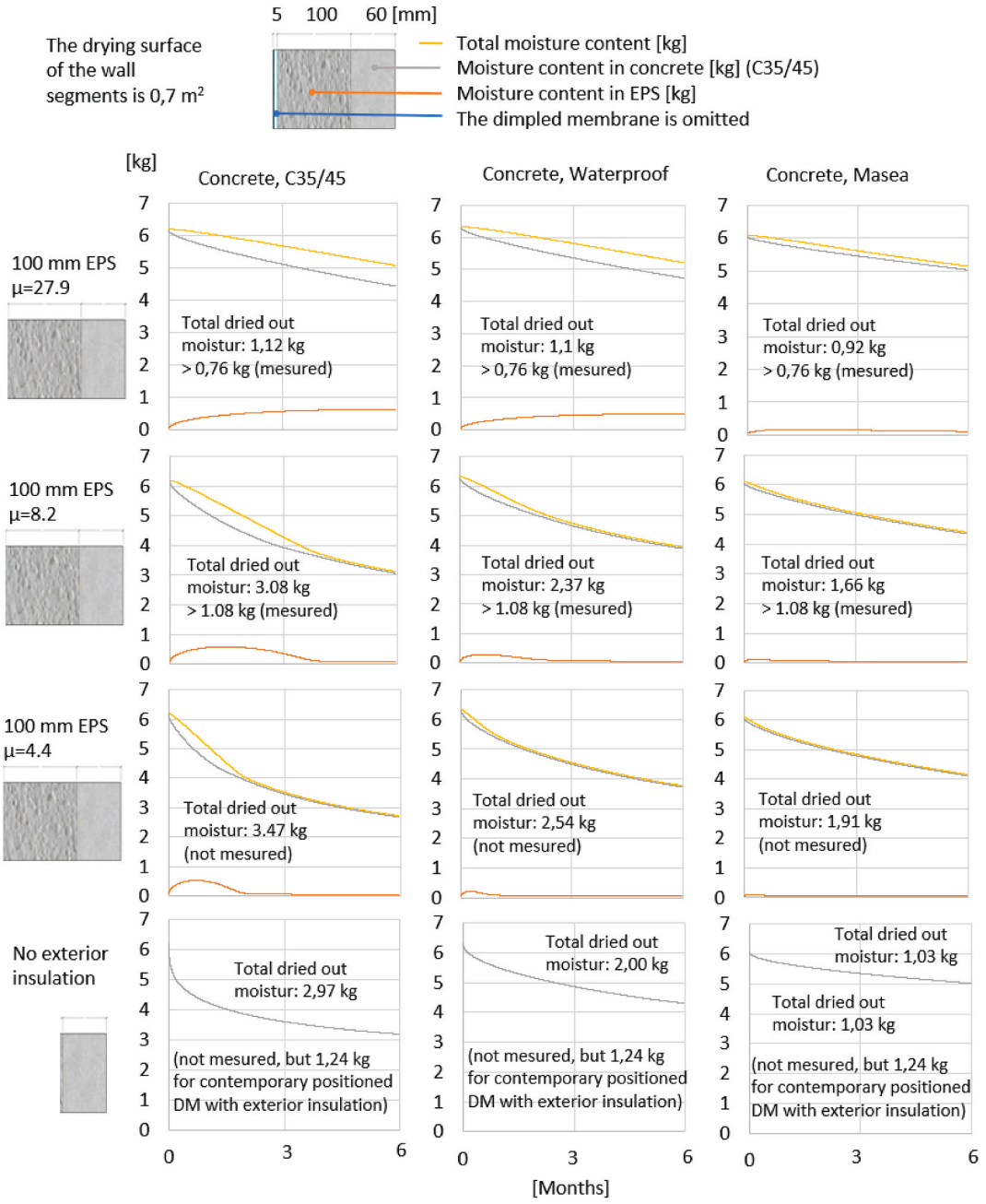

Fig. D1. *Simulated decrease in MC in concrete wall segments over a period of six months for thermal insulations with three different water vapour diffusion resistance factors (μ), and three concrete types. The air in the cold chamber had 80% RH/5°C; the air in the war chamber was 20% RH/20°C. The total amount of dried out moisture is compared to the amount of moisture dried out in the laboratory study* [10].

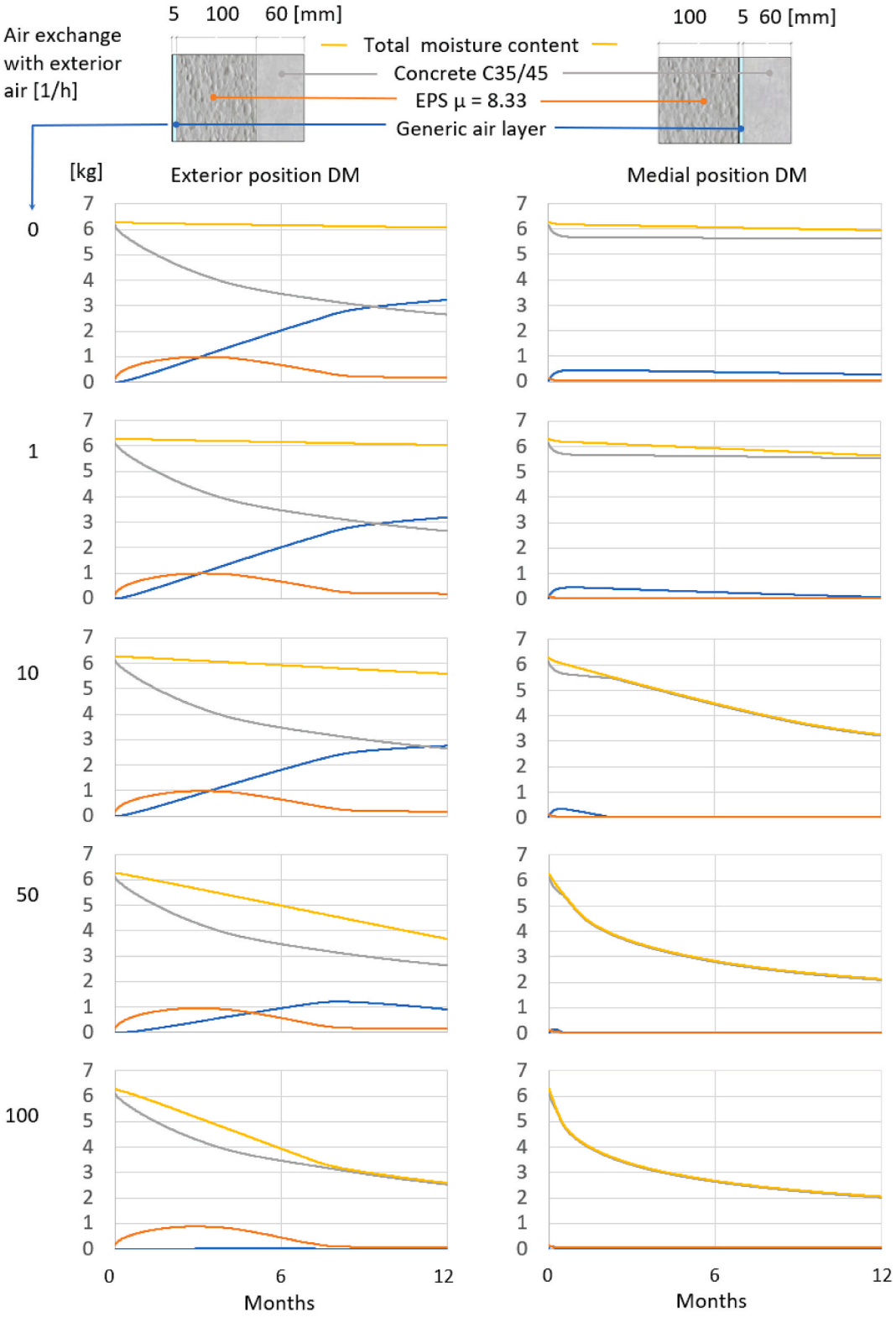

Fig. D2. MC decrease in concrete wall segments for various air exchange rates in the air gap behind the dimpled membrane (DM). The air in the cold chamber was 80% RH/5°C; the air in the war chamber was 20% RH/20°C.

References

[1] H. Viitanen, J. Vinha, K. Salminen, T. Ojanen, R. Peuhkuri, L. Paajanen, K. Lähdesmäki, Moisture and bio-deterioration risk of building materials and structures, J. Build. Phys. 33 (2010) 201–224, https://doi.org/10.1177/1744259109343511.

[2] S. Cai, B. Zhang, L. Cremaschi, Review of moisture behavior and thermal performance of polystyrene insulation in building applications, Build. Environ. 123 (2017) 50–65, https://doi.org/10.1016/j.buildenv.2017.06.034.

[3] S. Cai, B. Zhang, L. Cremaschi, Moisture behavior of polystyrene insulation in below-grade application, Energy Build. 159 (2018) 24–38, https://doi.org/10.1016/j.enbuild.2017.10.067.

[4] M. Jerman, R. Cerny, Effect of moisture content on heat and moisture transport and storage properties of thermal insulation materials, Energy Build. 53 (2012) 39–46, https://doi.org/10.1016/j.enbuild.2012.07.002.

[5] S.K. Asphaug, T. Kvande, B. Time, R.H. Peuhkuri, T. Kalamees, P. Johansson, U. Berardi, J. Lohne, Moisture control strategies of habitable basements in cold climates, Build. Environ. 169 (2020), 106572, https://doi.org/10.1016/j.buildenv.2019.106572.

[6] I. Hanssen-Bauer, E.J. Førland, I. Haddeland, H. Hisdal, S. Mayer, A. Nesje, J.E. Ø. Nilsen, S. Sandven, A.B. SandØ, A. Sortberg, B. Adlansvik, Climate in Norway 2100 - a Knowledge Base for Climate Adaptation, Norwegian Environment Agency, 2017. www.miljodirektoratet.no/M741. (Accessed 24 September 2021).

[7] V. Masson-Delmotte, A. Pirani, Y. Chen, J.B.R. Matthews, O. Yelekçi, et al., Climate Change 2021 the Physical Science Basis, Intergovernmental Panel on Climate Change, Switzerland, 2021. https://www.ipcc.ch/report/ar6/wg1/downloads/report/IPCC_AR6_WGI_SPM_final.pdf.

[8] J. Bonneau, T.D. Fletcher, J.F. Costelloe, M.J. Burns, Stormwater infiltration and the 'urban karst' – a review, J. Hydrol. 552 (2017) 141–150, https://doi.org/10.1016/j.jhydrol.2017.06.043.

[9] J. Straube, Field monitoring and hygrothermal modeling of interior basement insulation systems. https://www.buildingscience.com/documents/reports/rr-0906-field-monitoring-hygrothermal-modeling-basement-insulation/view, 2009. (Accessed 4 November 2020).

[10] S. Asphaug, I. Hjermann, B. Time, T. Kvande, Monitoring outward drying of externally insulated basement walls: a laboratory experiment, Build. Environ. 217 (2022), https://doi.org/10.1016/j.buildenv.2022.109097, 109097.

[11] S. Geving, P. Blom, M. Kvalvik, E. Martinsen, Utbedring Av Fuktskadede Kjelleryttervegger. Delrapport 2 - Felt-, Laboratorie- Og Beregningsmessige Undersøkelser Av Tre Metoder, SINTEF Bokhandel, 2011. https://www.sintefbok.no/book/index/918/utbedring_av_fuktskadede_kjelleryttervegger. (Accessed 4 November 2020).

[12] S. Pallin, Risk Assessment of Hygrothermal Performance - Building Envelop Retrofit, Doctoral Thesis, Chalmers University of Technology, 2013. http://publications.lib.chalmers.se/records/fulltext/177128/177128.pdf.

[13] J. Arfvidsson, L.-E. Harderup, I. Samuelson, Fukthandbok: Praktik och teori (Handbook in moisture: practice and theory), in: Fukthandbok, AB Svensk Byggtjanst, AB Svensk Byggtjanst, 2017.

[14] M.H. Hansen, E. Brandt, M. Vesterløkke, N. Okkels, Kældervægge og -gulve – fugtsikring og varmeisolering (basement walls and floors - moisture control and thermal insulation), Byg-Erfa. 19 (2015), 151114.

[15] P. Blom, S. Uvsløkk, Yttervegger mot terreng. Varmeisolering og tetting (Exterior walls below grade, Thermal insulation and sealing) The SINTEF Building Research Design Guides nr 523 (111) (2015). https://www.byggforsk.no/dokument/3304/yttervegger_mot_terreng_varmeisolering_og_tetting.

[16] N.R. Canada, Keeping the Heat in - section 6: basement insulation: floors, walls and crawl spaces. https://www.nrcan.gc.ca/energy-efficiency/homes/make-your-home-more-energy-efficient/keeping-the-heat/section-6-basement-insulation-floors-walls-and-crawl-spaces/15639, 2021. (Accessed 2 March 2022).

[17] M.C. Swinton, T. Kesik, Performance Guidelines for Basement Envelope Systems and Materials, National Research Council of Canada (NRC), Canada, 2005. http://citeseerx.ist.psu.edu/viewdoc/download?doi=10.1.1.138.1692&rep=rep1&type=pdf.

[18] E. Eesti, Moisture in Buildings (Niiskus Hoonetes) ET-2 0405-0497, 2003.

[19] J. Lstiburek, Understanding basements, ASHRAE J. 48 (2006) 24–29.

[20] J. Lahdensivu, I. Weijo, T. Turunen, S. Ahola, E. Sistonen, C. Vornanen-Winqvist, P. Annila, Reparation av fukt- och mikrobskadade byggnader. https://julkaisut.valtioneuvosto.fi/handle/10024/162010, 2020. (Accessed 11 March 2022).

[21] S. Geving, M. Kvalvik, E. Martinsen, Rehabilitation of basement walls with moisture problems by the use of vapour open exterior thermal insulation, in: Proceedings of the 9th Nordic Symposium on Building Physics, NSB 2011, Tampere University of Technology, 2011, pp. 323–330. https://app.cristin.no/results/show.jsf?id=806899.

[22] T. Kvande, Fuktsikre Konstruksjoner Mor Grunnen. Klima2050 Note 100, Trondheim, 2020. https://www.klima2050.no/klima-2050-note.

[23] P. Blom, Isolering Og Fuktsikring Av Yttervegger Mot Terreng. Målinger I Forsøksvegg. (Thermal Insulation and Moisture Control of Exterior Walls below Grade. Measurements in Experimental Walls), SINTEF akademisk forlag, 2012.

[24] J. Straube, The role of small gaps behind wall claddings on drainage and drying, in: 11th Canadian Conference on Building Science & Technology, Banff, Alberta, 2007.

[25] J. Straube, J. Smegal, Modeled and measured drainage, storage and drying behind cladding systems. https://www.buildingscience.com/documents/reports/rr-0905-modeled-measured-drainage-thermal-x/view, 2009. (Accessed 3 March 2022).

[26] G. Finch, J. Straube, in: Clearwater Beach (Ed.), Ventilated Wall Claddings: Review, Field Performance, and Hygrothermal Modeling, FL, USA, 2007, p. 16. https://wufi.de/literatur/Finch,%20Straube%202007%20-%20Ventilated%20Wall%20Claddings.pdf.

[27] J.F. Straube, R. van Straaten, E. Burnett, Field studies of ventilation drying, in: Buildings IX Proceedings, Oak Ridge National Laboratory, 2004.

[28] M. Rahiminejad, D. Khovalyg, Review on ventilation rates in the ventilated air-spaces behind common wall assemblies with external cladding, Build. Environ. 190 (2021), 107538, https://doi.org/10.1016/j.buildenv.2020.107538.

[29] H.H. Saber, W. Maref, M.C. Swinton, Thermal response of basement wall systems with low-emissivity material and furred airspace, J. Build. Phys. 35 (2012) 353–371, https://doi.org/10.1177/1744259111411652.

[30] L.F. Goldberg, A.C. Harmon, Cold Climate Foundation Retrofit Experimental Hygrothermal Performance: Cloquet Residential Research Facility Laboratory Results, 2015.

[31] F. Fedorik, R. Heiskanen, A. Laukkarinen, J. Vinha, Impacts of multiple refurbishment strategies on hygrothermal behaviour of basement walls, J. Build. Eng. 26 (2019), https://doi.org/10.1016/j.jobe.2019.100902.

[32] P. Blom, S.B. Holøs, Moisture content in insulated basement walls, in: Proceedings of the 8th Nordic Symposium on Building Physic, 2008. Copenhagen.

[33] M.C. Swinton, W. Maref, M.T. Bomberg, M.K. Kumaran, N. Normandin, In situ performance evaluation of spray polyurethane foam in the exterior insulation basement system (EIBS), Build. Environ. 41 (2006) 1872–1880, https://doi.org/10.1016/j.buildenv.2005.06.028.

[34] Fraunhofer IBP, WUFI®Pro (n.d.), https://wufi.de/en/. (Accessed 17 August 2021).

[35] C. Bost, How to Model Heat and Moisture Transport in Porous Media with COMSO®, COMSOL Blog, 2017. https://www.comsol.com/blogs/how-to-model-heat-and-moisture-transport-in-porous-media-with-comsol/. (Accessed 21 August 2021).

[36] S.K. Asphaug, B. Time, T. Kvande, Hygrothermal simulations of thermally insulated basement envelopes - importance of boundary conditions below grade, Build. Environ. 199 (2021), 107920, https://doi.org/10.1016/j.buildenv.2021.107920.

[37] S.K. Asphaug, B. Time, T. Kvande, Moisture accumulation in building Façades exposed to accelerated artificial climatic ageing—a complementary analysis to NT build 495, Buildings 11 (2021) 568, https://doi.org/10.3390/buildings11120568.

[38] H.M. Künzel, Simultaneous Heat and Moisture Transport in Building Components: One- and Two-Dimensional Calculation Using Simple Parameters, IRB-Verlag, Stuttgart, 1995.

[39] C. Bost, How to Model Heat and Moisture Transport in Air with COMSOL®, COMSOL, 2017 (accessed April 29, 2022), https://www.comsol.com/blogs/how-to-model-heat-and-moisture-transport-in-air-with-comsol/.

[40] S. Geving, Moisture Design of Building Constructions. Hygrothermal Analysis Using Simulation Models. Part I, Norwegian University of Science and Technology (NTNU), 1997.

[41] NS-EN ISO 13788:2012, Hygrothermal Performance of Building Components and Building Elements - Internal Surface Temperature to Avoid Critical Surface Humidity and Interstitial Condensation - Calculation Methods, 2012.

[42] NS-EN 15026:2007, Hygrothermal performance of building components and building elements - assessment of moisture transfer by numerical simulation. https://www.standard.no/no/Nettbutikk/produktkatalogen/Produktpresentasjon/?ProductID=271232, 2007. (Accessed 4 November 2020).

[43] H. Janssen, J. Carmeliet, H. Hens, The influence of soil moisture transfer on building heat loss via the ground, Build. Environ. 39 (2004) 825–836, https://doi.org/10.1016/j.buildenv.2004.01.004.

[44] H. Janssen, J. Carmeliet, H. Hens, The influence of soil moisture in the unsaturated zone on the heat loss from buildings via the ground, JTEBS 25 (2002), https://doi.org/10.1177/0075424202025004683.

[45] NS-EN ISO 13793:2001, Bygningers Termiske Egenskaper - Termisk Dimensjonering Av Fundamenter for a Unnga Telehiv, 2001.

[46] M. Saaly, K. Bobko, P. Maghoul, M. Kavgic, H. Holländer, Energy performance of below-grade envelope of an institutional building in cold regions, J. Build. Eng. 27 (2020), https://doi.org/10.1016/j.jobe.2019.100911.